

Deep Contrastive Learning is Provably (almost) Principal Component Analysis

Yuandong Tian¹

Abstract

We show that Contrastive Learning (CL) under a family of loss functions (including InfoNCE) has a game-theoretical formulation, where the *max player* finds representation to maximize contrastiveness, and the *min player* puts weights on pairs of samples with similar representation. We show that the max player who does *representation learning* reduces to Principal Component Analysis for deep linear network, and almost all local minima are global, recovering optimal PCA solutions. Experiments show that the formulation yields comparable (or better) performance on CIFAR10 and STL-10 when extending beyond InfoNCE, resulting in novel contrastive losses. Furthermore, we extend our theoretical analysis to 2-layer ReLU networks, showing its sharp difference from linear ones, and proving that feature composition is preferred over picking single dominant feature under strong augmentation.

1. Introduction

While contrastive self-supervised learning has been shown to learn good features (Chen et al., 2020; He et al., 2020; Oord et al., 2018), and in many cases comparable with features learned from supervised learning, it remains an open problem what feature it learns, in particular when deep nonlinear network is used. Theory on this is quite sparse, mostly focusing on loss function (Arora et al., 2019) and treat the networks as a black-box function approximator.

In this paper, we present a *game-theoretical* view for contrastive learning (CL): the gradient descent of a family of contrastive loss functions $\mathcal{L}(\theta)$ corresponds to a min-max iterative procedure (Fig. 1) on an energy function $\mathcal{E}_\alpha(\theta)$ plus a regularization $\mathcal{R}(\alpha)$. In this view, the *max player* θ learns a representation to maximize the contrastiveness of different samples and keep different augmentation view of the same sample similar, while the *min player* α puts more weights on pairs of different samples that are similar in the representation space, subject to regularization. Empirically,

¹Meta AI Research. Correspondence to: Yuandong Tian <yuan-dong@fb.com>.

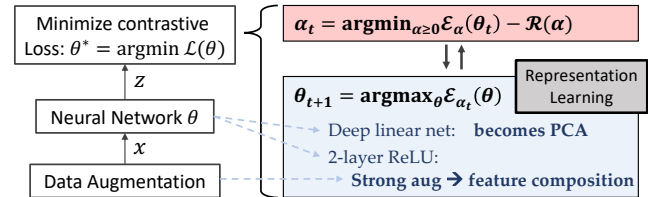


Figure 1. We open the blackbox of contrastive learning (CL) by studying the interplay among the contrastive loss, neural network architectures and data augmentation. **Our main contribution:** minimizing popular contrastive loss \mathcal{L} (e.g., InfoNCE) is equivalent to a min-max optimization procedure on an energy function $\mathcal{E}_\alpha(\theta)$ with regularization $\mathcal{R}(\alpha)$, in which the *max player* θ finds representations to maximize contrastiveness, while the *min player* α finds sample pairs with minimal contrastiveness. Furthermore, under deep linear network, the max player who does representation learning is equivalent to Principal Component Analysis (PCA). In 2-layer ReLU case, one major finding is that strong augmentation leads to feature composition.

this formulation with various regularization terms leads to novel loss functions and our experiments show comparable (or better) performance in CIFAR10 (Krizhevsky et al., 2009) and STL-10 (Coates et al., 2011).

We then focus on the behavior of the max player who does *representation learning* via maximizing the energy function $\mathcal{E}_\alpha(\theta)$. When the underlying network is deep linear, we show that $\max_{\theta} \mathcal{E}_\alpha(\theta)$ is exactly the loss function (under re-parameterization) of Principal Component Analysis (PCA) (Wold et al., 1987), a century-old unsupervised dimension reduction method. To further show they are equivalent, we prove that the nonlinear training dynamics of CL with linear multi-layer feedforward network (MLP) has nice properties: with properly weight normalization, almost all its local optima are global, achieving optimal PCA objective. The only difference here is that, the data augmentation provides negative eigen-directions to avoid.

Furthermore, we extend our analysis to 2-layer ReLU network, to explore the difference between the PCA solution and the solution learned by nonlinear network. Assuming the data follow an orthogonal mixture model, the 2-layer ReLU networks enjoy similar dynamics as the linear one, except for a special *sticky weight rule* that keeps the low-layer weights to be non-negative and stays zero when touching

zero. In the case of one hidden node, we prove that the solution in ReLU always picks a single mode from the mixtures. In the case of multiple hidden nodes with disjoint receptive fields, we prove that weight solutions that capture *feature compositionality* are more favorable than solutions that capture a single dominant feature under strong augmentation, addressing empirical puzzles (Chen et al., 2021; Tian et al., 2020b) that strong data augmentation seems to be the key for self-supervised learning to work.

2. Related Work

Contrastive learning. While many contrastive learning techniques (e.g., SimCLR (Chen et al., 2020), MoCo (He et al., 2020), PIRL (Misra & Maaten, 2020), SwAV (Caron et al., 2020), DeepCluster (Caron et al., 2018), Barlow Twins (Zbontar et al., 2021), InstDis (Wu et al., 2018), etc) have been proposed empirically and able to learn good representations for downstream tasks, theoretical study is relatively sparse, mostly focusing on loss function itself (Tian et al., 2020b; HaoChen et al., 2021; Arora et al., 2019), e.g., the relationship of loss functions with mutual information (MI). To our knowledge, there is no analysis that combines the property of neural network and that of loss functions.

Theoretical analysis of deep networks. Many works focus on analysis of deep linear networks in supervised setting, where label is given. (Baldi & Hornik, 1989; Zhou & Liang, 2018; Kawaguchi, 2016) analyze the critical points of linear networks. (Saxe et al., 2014; Arora et al., 2018) also analyze the training dynamics. On the other hand, analyzing nonlinear networks has been a difficult task. Existing works mostly lie in supervised learning, e.g., teacher-student setting (Tian, 2020; Allen-Zhu et al., 2018), landscape (Safran & Shamir, 2018). For contrastive learning, recent work (Wen & Li, 2021) analyzes the dynamics of 1-layer ReLU networks with a specific weight structure, and (Jing et al., 2022) analyzes the collapsing behaviors in 2-layer linear network for CL. To our best knowledge, we are not aware of such analysis on deep networks (> 2 layers, linear or nonlinear) in the context of CL.

Game-theoretical formulation and Principal Component Analysis (PCA). EigenGame (Gemp et al., 2021) reformulates PCA itself as a multi-player competitive game. (Lee et al., 2021) establishes the statistical connection between non-linear Canonical Component Analysis (CCA) and SimSiam (Chen & He, 2020) for any zero-mean encoder, without considering the aspect of training dynamics. In contrast, we reformulate contrastive learning as a game, in which the max player is a reparameterization of PCA, optimized with gradient descent, and analyze its property when the encoder has certain neural architectures.

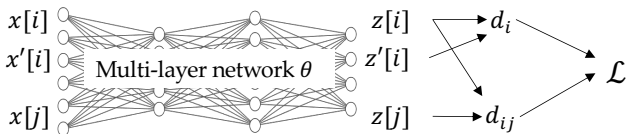


Figure 2. Problem Setting. Data points (i -th sample $\mathbf{x}[i]$ and its augmented version $\mathbf{x}[i']$, j -th sample $\mathbf{x}[j]$) are sent to networks with weights θ , to yield outputs $\mathbf{z}[i]$, $\mathbf{z}[i']$ and $\mathbf{z}[j]$. From the outputs, we compute pairwise distance $d_{ij} := \|\mathbf{z}[i] - \mathbf{z}[j]\|_2^2/2$ and intra-class distance $d_i := \|\mathbf{z}[i] - \mathbf{z}[i']\|_2^2/2$ and performs contrastive learning with objective function (Eqn. 1).

Contrastive Loss	$\phi(x)$	$\psi(x)$
InfoNCE (Oord et al., 2018)	$\tau \log(\epsilon + x)$	$e^{x/\tau}$
MINE (Belghazi et al., 2018)	$\log(x)$	e^x
Triplet (Schroff et al., 2015)	x	$[x + \epsilon]_+$
Soft Triplet (Tian et al., 2020c)	$\tau \log(1 + x)$	$e^{x/\tau + \epsilon}$
N+1 Tuplet (Sohn, 2016)	$\log(1 + x)$	e^x
Lifted Structured (Oh Song et al., 2016)	$[\log(x)]_+^2$	$e^{x+\epsilon}$
Modified Triplet Eqn. 10 (Coria et al., 2020)	x	$\text{sigmoid}(cx)$
Triplet Contrastive Eqn. 2 (Ji et al., 2021)	linear	linear

Table 1. A general family of contrastive loss $\mathcal{L}_{\phi, \psi}$ (Eqn. 1). Different existing loss functions corresponds to different monotonous functions ϕ and ψ . Here $[x]_+ := \max(x, 0)$.

3. A Min-max View of Contrastive Loss

Notation. Suppose we have N pairs of samples $\{\mathbf{x}[i]\}_{i=1}^N$ and $\{\mathbf{x}[i']\}_{i=1}^N$. Both $\mathbf{x}[i]$ and $\mathbf{x}[i']$ are augmented samples from sample i and \mathbf{x} represents the input batch. These samples are sent to neural networks and $\mathbf{z}[i]$ and $\mathbf{z}[i']$ are their outputs. The goal of contrastive learning (CL) is to find the representation to maximize the distance $d_{ij} := \|\mathbf{z}[i] - \mathbf{z}[j]\|_2^2/2$ between distinct samples i and j , and minimize the distance $d_i := \|\mathbf{z}[i] - \mathbf{z}[i']\|_2^2/2$ between different data augmentations $\mathbf{x}[i]$ and $\mathbf{x}[i']$ of the same sample i .

3.1. A general class of contrastive loss

We consider minimizing a general family of loss functions $\mathcal{L}_{\phi, \psi}$, where ϕ and ψ are monotonously increasing and differentiable scalar functions that parameterize the loss:

$$\min_{\theta} \mathcal{L}_{\phi, \psi}(\theta) := \sum_{i=1}^N \phi \left(\sum_{j \neq i} \psi(d_i - d_{ij}) \right) \quad (1)$$

Here both i and j run from 1 to N . With different ϕ and ψ , Eqn. 1 covers many loss functions (Tbl. 1). In particular, setting $\phi(x) = \tau \log(\epsilon + x)$ and $\psi(x) = \exp(x/\tau)$ gives a generalized version of InfoNCE loss (Oord et al., 2018):

$$\mathcal{L}_{nce} := -\tau \sum_{i=1}^N \log \frac{\exp(-d_i/\tau)}{\epsilon \exp(-d_i/\tau) + \sum_{j \neq i} \exp(-d_{ij}/\tau)} \quad (2)$$

where $\epsilon > 0$ is some constant not related to $\mathbf{z}[i]$ and $\mathbf{z}[i']$. $\epsilon = 1$ has been used in many works (He et al., 2020; Tian et al., 2020a). Setting $\epsilon = 0$ yields SimCLR set-

ting (Chen et al., 2020) where the denominator doesn't contain $\exp(-d_i/\tau)$. This is also used in (Yeh et al., 2021).

3.2. The other side of gradient descent of contrastive loss

To minimize $\mathcal{L}_{\phi,\psi}$, gradient descent follows its negative gradient direction. As a first discovery of this work, it turns out that the gradient descent of the loss function \mathcal{L} is the *gradient ascent* direction of another energy function \mathcal{E}_α :

Theorem 1. *For any differential mapping $\mathbf{z} = \mathbf{z}(\mathbf{x}; \boldsymbol{\theta})$, gradient descent of $\mathcal{L}_{\phi,\psi}$ is equivalent to **gradient ascent** of the objective $\mathcal{E}_\alpha(\boldsymbol{\theta}) := \text{tr}(\mathbb{C}_\alpha[\mathbf{z}(\boldsymbol{\theta}), \mathbf{z}(\boldsymbol{\theta})])$:*

$$\frac{\partial \mathcal{L}_{\phi,\psi}}{\partial \boldsymbol{\theta}} = -\frac{1}{2} \frac{\partial \mathcal{E}_\alpha}{\partial \boldsymbol{\theta}} \Big|_{\alpha=\alpha(\boldsymbol{\theta})} \quad (3)$$

Here the pairwise importance $\alpha = \alpha(\boldsymbol{\theta}) := \{\alpha_{ij}(\boldsymbol{\theta})\}$ is a function of input batch \mathbf{x} , defined as:

$$\alpha_{ij} := \phi' \left(\sum_{j \neq i} \psi(d_i - d_{ij}) \right) \psi'(d_i - d_{ij}) \geq 0 \quad (4)$$

where $\phi', \psi' \geq 0$ are derivatives of ϕ, ψ . The contrastive covariance $\mathbb{C}_\alpha[\cdot, \cdot]$ is defined as (here $\beta_i := \sum_{j \neq i} \alpha_{ij}$):

$$\begin{aligned} \mathbb{C}_\alpha[\mathbf{a}, \mathbf{b}] &:= \sum_{i \neq j} \alpha_{ij} (\mathbf{a}[i] - \mathbf{a}[j]) (\mathbf{b}[i] - \mathbf{b}[j])^\top \\ &- \sum_{i=1}^N \beta_i (\mathbf{a}[i] - \mathbf{a}[i']) (\mathbf{b}[i] - \mathbf{b}[i'])^\top \end{aligned} \quad (5)$$

Please check Supplementary Materials (SM) for all proofs.

From the definition of energy $\mathcal{E}_\alpha(\boldsymbol{\theta})$, it is clear that α_{ij} determines the importance of each sample pair $\mathbf{x}[i]$ and $\mathbf{x}[j]$. For (i, j) -pair that ‘‘deserves attention’’, α_{ij} is large so that it plays a large role in the contrastive covariance term. In particular, for InfoNCE loss with $\epsilon = 0$, the pairwise importance α takes the following form:

$$\alpha_{ij} = \frac{\exp(-d_{ij}/\tau)}{\sum_{j \neq i} \exp(-d_{ij}/\tau)} > 0, \quad \beta_i \equiv 1 \quad (6)$$

which means that InfoNCE focuses on (i, j) -pair with small distance d_{ij} . If both ϕ and ψ are linear, \mathcal{L} is a simple subtraction of positive/negative distances and $\alpha_{ij} = \text{const.}$

From Thm. 1, an important observation is that when evaluating the gradient of \mathcal{E}_α , α does not go through backpropagation w.r.t. $\boldsymbol{\theta}$. In fact, in Sec. 6.1 we show that adding gradient through $\alpha(\boldsymbol{\theta})$ yields worse empirical performance. This suggests that α can be treated as an *independent* variable. It turns out that for InfoNCE, this is indeed the case and α can be determined by a separate optimization process:

Theorem 2. *For InfoNCE loss \mathcal{L}_{nce} with $\epsilon = 0$, the corresponding pairwise importance α (Eqn. 6) is the solution to the minimization problem:*

$$\min_{\alpha \geq 0} \mathcal{E}_\alpha(\boldsymbol{\theta}) - \mathcal{R}(\alpha),$$

with the constraint $\sum_{j \neq i} \alpha_{ij} = 1$. Here the regularization $\mathcal{R}(\alpha)$ is the entropy: $\mathcal{R}(\alpha) = \mathcal{R}_H(\alpha) := 2\tau \sum_{i=1}^N H(\alpha_i) = -2\tau \sum_{i=1}^N \sum_{j \neq i} \alpha_{ij} \log \alpha_{ij}$.

This leads to a novel *game-theoretical* formulation for CL:

Corollary 1. *The minimization of InfoNCE loss \mathcal{L}_{nce} with $\epsilon = 0$ is equivalent to coordinate-wise optimization to the max-min objective $\max_{\boldsymbol{\theta}} \min_{\alpha \geq 0} \mathcal{E}_\alpha(\boldsymbol{\theta}) - \mathcal{R}(\alpha)$:*

$$\mathcal{P}_g : \quad \begin{aligned} \alpha_t &= \arg \min_{\alpha \geq 0} \mathcal{E}_\alpha(\boldsymbol{\theta}_t) - \mathcal{R}(\alpha) \\ \boldsymbol{\theta}_{t+1} &= \arg \max_{\boldsymbol{\theta}} \mathcal{E}_{\alpha_t}(\boldsymbol{\theta}) \end{aligned} \quad (7)$$

Furthermore, we optimize α analytically (i.e., one step to optimal) while performing one-step gradient ascent for $\boldsymbol{\theta}$.

Intuitively, the ‘‘max player’’ $\boldsymbol{\theta}$, which is the *representation learning* component of CL, learns a representation to maximize the distance of different samples and minimize the distance of the same sample with different augmentations (as suggested by $\mathbb{C}_\alpha[\mathbf{z}, \mathbf{z}]$); while the ‘‘min player’’ α assigns high weights (with proper regularization) on confusion pairs for ‘‘max player’’ to solve.

From this formulation, different pairwise importance α corresponds to different loss functions within the loss family specified by Eqn. 1, and choosing among this family (i.e., different ϕ and ψ) can be regarded as choosing different α when optimizing the *same* objective $\mathcal{E}_\alpha(\boldsymbol{\theta})$. α can be determined either directly or by specifying a regularizer $\mathcal{R}(\alpha)$. This potentially opens a novel revenue for CL loss design.

We have conducted initial experiments (Sec. 6.1), showing that the min-max formulation \mathcal{P}_g gives comparable (or even better) downstream performance in CIFAR10 and STL-10, compared to vanilla InfoNCE loss.

While many previous works (Kalantidis et al., 2020; Robinson et al., 2021) focus on seeking and putting more weights on hard samples, Corollary 1 shows that contrastive losses already have such mechanism at the batch level, focusing on ‘‘hard-negative pairs’’ beyond hard-negative samples.

4. Representation Learning in Deep Linear CL is Principal Component Analysis

For the coordinate-wise optimization procedure (Eqn. 28), optimizing over α is well-understood, since $\mathcal{E}_\alpha(\boldsymbol{\theta})$ is *linear* w.r.t. α and $\mathcal{R}(\alpha)$ in general is a (strong) concave function. As a result, α has a unique optimal. On the other hand, understanding the max player $\max_{\boldsymbol{\theta}} \mathcal{E}_\alpha(\boldsymbol{\theta})$ is important since

it performs *representation learning* in CL. It is also a hard problem because of non-convex optimization.

We start with a specific case when \mathbf{z} is a deep linear network, i.e., $\mathbf{z} = W(\boldsymbol{\theta})\mathbf{x}$, where W is the equivalent linear mapping for the deep linear network, and $\boldsymbol{\theta}$ is the parameters to be optimized. Note that this covers many different kinds of deep linear networks, including VGG-like (Saxe et al., 2014), ResNet-like (Hardt & Ma, 2017) and DenseNet-like (Huang et al., 2017). For notation convenience, in the following we define $\mathbb{C}_\alpha[\mathbf{x}] := \mathbb{C}_\alpha[\mathbf{x}, \mathbf{x}]$.

Corollary 2 (Representation learning in Deep Linear CL reparameterizes PCA). *When $\mathbf{z} = W(\boldsymbol{\theta})\mathbf{x}$ with a constraint $WW^\top = I$, \mathcal{E}_α is the objective of Principal Component Analysis (PCA) with reparameterization $W = W(\boldsymbol{\theta})$:*

$$\max_{\boldsymbol{\theta}} \mathcal{E}_\alpha(\boldsymbol{\theta}) = \text{tr}(W(\boldsymbol{\theta})X_\alpha W^\top(\boldsymbol{\theta})) \quad \text{s.t. } WW^\top = I \quad (8)$$

here $X_\alpha := \mathbb{C}_\alpha[\mathbf{x}]$ is the contrastive covariance of input \mathbf{x} .

As a comparison, in traditional Principal Component Analysis, the objective is (Kokopoulou et al., 2011):

$$\max_W \text{tr}(WV[\mathbf{x}]W^\top) \quad \text{s.t. } WW^\top = I \quad (9)$$

To see why $X_\alpha = \mathbb{C}_\alpha[\mathbf{x}]$ is similar to covariance matrix $V[\mathbf{x}]$ in PCA¹, just notice that if $\alpha_{ij} = 1/2N(N-1)$ (e.g., with linear ϕ and ψ) and there is no data augmentation (so that $\mathbf{x}[i] = \mathbf{x}[i']$), then $X_\alpha \rightarrow V[\mathbf{x}]$ when $N \rightarrow +\infty$. In the case of supervised CL (i.e., pairs from the same/different labels are treated as positive/negative (Khosla et al., 2020)), then it is connected with Fisher’s Linear Discriminant Analysis (Fisher, 1936).

Here we show a mathematically rigorous connection between CL and dimensional reduction, as suggested intuitively in (Hadsell et al., 2006). Unlike traditional PCA, due to the presence of data augmentation, while symmetric, the contrastive covariance X_α is not necessarily a PSD matrix. Nevertheless, the intuition is the same: to find the direction that corresponds to maximal variation of the data.

While it is interesting to discover that CL with deep linear network is essentially a reparameterization of PCA, it remains elusive that such a reparameterization leads to the same solution of PCA, in particular when the network is deep (and may contain local optima). Also, PCA has an overall end-to-end constraint $WW^\top = I$, while in network training, we instead use normalization layers and it is unclear whether they are equivalent or not.

In this section, we show for a specific deep linear model, almost all its local maxima of Eqn. 29 are global and it indeed solves PCA.

¹Here $V[\mathbf{x}] := \mathbb{E}[(\mathbf{x} - \mathbb{E}[\mathbf{x}])^2]$ is the covariance matrix, if we treat \mathbf{x} as a d -dimensional random variable.

4.1. A concrete deep linear model

We study a concrete deep linear network with parameters/weights $\boldsymbol{\theta} := \{W_l\}_{l=1}^L$:

$$\mathbf{z}[i] := W_L W_{L-1} \dots W_1 \mathbf{x}[i] \quad (10)$$

Here $W_l \in \mathbb{R}^{n_l \times n_{l-1}}$, n_l is the number of nodes at layer l , $\mathbf{z}[i]$ is the output of $\mathbf{x}[i]$ and similarly $\mathbf{z}[i']$ for $\mathbf{x}[i']$. We use $\boldsymbol{\theta}$ to represent the collection of weights at all layers. For convenience, we define the l -th layer activation $\mathbf{f}_l[i] = W_l \mathbf{f}_{l-1}[i]$. With this notation $\mathbf{f}_0[i] = \mathbf{x}[i]$ is the input and $\mathbf{z}[i] = W_L \mathbf{f}_{L-1}[i]$.

We call this setting `DeepLin`. The Jacobian matrix $W_{>l} := W_L W_{L-1} \dots W_{l+1}$ and $W := W_{>0} = W_L W_{L-1} \dots W_1$.

Lemma 1. *The training dynamics in `DeepLin` is:*

$$\dot{W}_l = W_{>l}^\top W_{>l} W_l \mathbb{C}_\alpha[\mathbf{f}_{l-1}] \quad (11)$$

Note that $\mathbb{C}_\alpha[\mathbf{f}_0] = \mathbb{C}_\alpha[\mathbf{x}] = X_\alpha$. Similar to supervised learning (Arora et al., 2018; Du et al., 2018b), nearby layers are also balanced: $\frac{d}{dt}(W_l W_l^\top - W_{l+1}^\top W_{l+1}) = 0$.

4.2. Normalization Constraints

Note that if we just run the training dynamics (Eqn. 30) without any constraints, $\|W_l\|_F$ will go to infinity. Fortunately, empirical works already suggest various ways of normalization to stabilize the network training.

One popular technique in CL is ℓ_2 normalization. It is often put right after the output of the network and before the loss function \mathcal{L} (Chen et al., 2020; Grill et al., 2020; He et al., 2020), i.e., $\hat{\mathbf{z}}[i] = \mathbf{z}[i]/\|\mathbf{z}[i]\|_2$. Besides, LayerNorm (Ba et al., 2016) (i.e., $\hat{\mathbf{f}}[i] = (\mathbf{f}[i] - \text{mean}(\mathbf{f}[i]))/\text{std}(\mathbf{f}[i])$) is extensively used in Transformer-based models (Xiong et al., 2020). Here we show that for gradient flow dynamics of MLP models, such normalization layers conserve $\|W_l\|_F$ for any l below it, regardless of loss function.

Lemma 2. *For MLP architecture, if the weight layer W_l is below a ℓ_2 -norm or LayerNorm layer, then $\frac{d}{dt}\|W_l\|_F^2 = 0$.*

Note that Lemma 2 also holds for nonlinear MLP with reversible activations, which includes ReLU (see SM).

Therefore, without loss of generality, we consider the following complete objective for max player with `DeepLin`:

$$\max_{\boldsymbol{\theta} \in \Theta} \mathcal{E}_\alpha(\boldsymbol{\theta}) := \text{tr}(W X_\alpha W^\top) \quad (12)$$

where Θ is the constraint set of the weights due to normalization:

$$\Theta := \{\boldsymbol{\theta} : \|W_l\|_F = 1, 1 \leq l \leq L\} \quad (13)$$

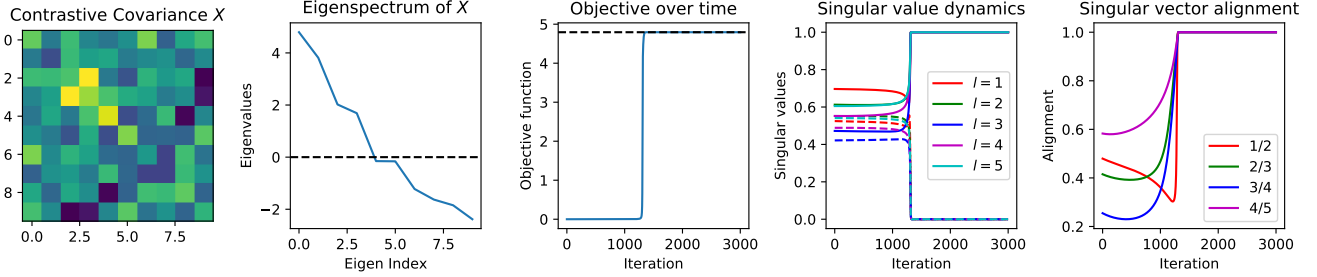


Figure 3. Dynamics of CL with multilayer ($L = 5$) linear network (DeepLin) with fixed α . Running the training dynamics (Eqn. 30) quickly leads to convergence towards the maximal eigenvalue of X_α . For dynamics of singular value of W_l , the largest singular values (solid lines) converges to 1 while the second largest singular values (dashed lines) decay to 0.

4.3. Representation Learning with DeepLin is PCA

As one of our main contribution, the following theorem asserts that almost all local optimal solutions of Eqn. 12 are global, and the optimal objective corresponds to the PCA objective. Note that (Kawaguchi, 2016; Laurent & Brecht, 2018) proves no bad local optima for deep linear network in supervised learning, while here we give similar results for CL, and additionally we also give the (simple) rank-1 structure of all local optima.

Theorem 3 (Representation Learning with DeepLin is PCA). *If $\lambda_{\max}(X_\alpha) > 0$, then for any local maximum $\theta \in \Theta$ of Eqn. 12 whose $W_{>1}^\top W_{>1}$ has distinct maximal eigenvalue:*

- there exists a set of unit vectors $\{v_l\}_{l=0}^L$ so that $W_l = v_l v_{l-1}^\top$ for $1 \leq l \leq L$, in particular, v_0 is the unit eigenvector corresponding to $\lambda_{\max}(X_\alpha)$;
- θ is global optimal with objective $\mathcal{E}^* = \lambda_{\max}(X_\alpha)$.

Remark. Here we prove that given fixed α , maximizing $\mathcal{E}_\alpha(\theta)$ gives rank-1 solutions for deep linear network. This conclusion is an extension of (Jing et al., 2022), which shows weight collapsing happens if θ is 2-layer linear network and α is fixed. If the pairwise importance α is adversarial as suggested in the game-theoretical framework, then it may not lead to a rank-1 solution. In fact, α can magnify minimal eigen-directions and change the eigenstructure of X_α continuously. We leave it for future work.

Compared to recent works (Ji et al., 2021) that also relates CL with PCA in linear representation setting using constant α , our Theorem 3 has no statistical assumptions on data distribution and augmentation, and operates on vanilla InfoNCE loss and deep architectures.

5. Representation Learning under ReLU nonlinearity in Two-layer Network

So far we have shown that the max player $\max_\theta \mathcal{E}_\alpha(\theta) := \text{tr}(\mathbb{C}_\alpha[z(\theta)])$ is essentially a PCA objective when the input-output mapping $z = W(\theta)x$ is linear. A natural question arises. What is the benefit of CL if its representation learning

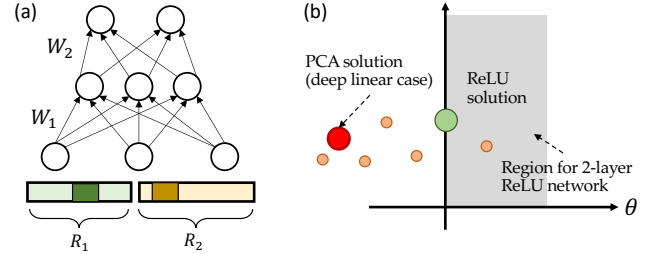


Figure 4. (a) We study 2-layer ReLU network under orthogonal mixture assumption (Assumption 1) that allows at most one positive entry in the input x per receptive field. (b) The dynamics of ReLU2Layer follows its linear counterpart plus *sticky weight rule* that sticks low-layer weights to non-negative regions (Thm. 4). Therefore, the PCA solution in the linear case may not be feasible/optimal for ReLU2Layer.

component has such a simple nature? Why can it learn a good representation in practice beyond PCA?

For this, nonlinearity is the key but understanding its role is highly nontrivial. For example, when the neural network model is nonlinear, Thm. 1 and Corollary 1 holds but *not* Corollary 2. Therefore, there is not even a well-defined X_α due to the fact that multiple hidden nodes can be switched on/off given different data input. Previous works (Safran & Shamir, 2018; Du et al., 2018a) also show that with nonlinearity, in supervised learning spurious local optima exist.

Here we take a first step to analyze nonlinear cases. We study 2-layer models with ReLU activation $h(x) = \max(x, 0)$. We show that with a proper data assumption, the 2-layer model shares a *modified* version of dynamics with its linear version, and the contrastive covariance term X_α (and its eigenstructure) remains well-defined and useful in nonlinear case. Given the setting, we show that with strong data augmentation, its fixed points with high energy \mathcal{E}_α encourages feature compositionality, consistent with existing empirical observations.

5.1. The 2-layer ReLU network and data model

We consider the bottom-layer weight $W_1 = [w_{11}, w_{12}, \dots, w_{1K}]^\top$ with w_{1k} being the k -th filter.

For brevity, let $K = n_1$ be the number of hidden nodes. Each filter w_{1k} may cover a different subset x_k of the input x . The subset R_k is called *receptive field*. We still consider solution in the constraint set Θ (Eqn. 13), since Lemma 2 still holds for ReLU networks. This model is named `ReLU2Layer`.

In addition, we assume the following data model:

Assumption 1 (Orthogonal mixture model within receptive field R_k). *For each receptive field R_k , there exists a set of orthonormal bases $\{\bar{x}_{k,m}\}_{m=1}^M$ so that any input data $x_k[i] = \sum_m a_{km}[i] \bar{x}_{k,m}$ satisfies the following property:*

- **Nonnegative:** $a_{km}[i] \geq 0$.
- **One-hot:** For at most one m , $a_{km}[i] > 0$.
- **Augmentation only scales x_k by a (sample-dependent) factor, i.e.,** $x_k[i'] = \gamma[i] x_k[i]$ with $\gamma[i] > 0$.

Since all x_k appears in the inner-product with the weight vectors w_{1k} , with a rotation of coordination, we can just set $\bar{x}_{k,m} = e_m$, where e_m is the one-hot vector with m -th component being 1. In this case, $x_k \geq 0$ is always a one-hot vector with only at most only one positive entry, and the notation $m \in R_k$ means that the *feature* m lies within the receptive field R_k .

Intuition of the model. Intuitively, the model only holds for small receptive field R_k of the input where x_k contains a bunch of *isolated* patterns, without any compositionality. As we will see, we only consider feature combination that happens only across different receptive fields (i.e., between x_k and $x_{k'}$ for $k \neq k'$), where features can *co-occur*.

With this assumption, we only need to consider nonnegative low-layer weights and X_α is still a valid quantity for `ReLU2Layer`:

Lemma 3 (Evaluation of `ReLU2Layer`). *If Assumption 1 holds, setting $w'_{1k} = \max(w_{1k}, 0)$ won't change the output of `ReLU2Layer`. Furthermore, if $W_1 \geq 0$, then the formula for linear network $\mathcal{E}_\alpha = \text{tr}(W_2 W_1 X_\alpha W_1^\top W_2^\top)$ still works for `ReLU2Layer`.*

On the other hand, sharing the energy function \mathcal{E}_α does not mean `ReLU2Layer` is completely identical to its linear version. In fact, the dynamics follows its linear counterparts, but with important modifications (Fig. 4(b)):

Theorem 4 (Dynamics of `ReLU2Layer`). *If Assumption 1 holds, then the dynamics of `ReLU2Layer` with $w_{1k} \geq 0$ is equivalent to linear dynamics with the **Sticky Weight rule**: any component that reaches 0 stays 0.*

As we will see, this modification leads to very different dynamics and local optima in `ReLU2Layer` from linear cases, even when there is only one ReLU node.

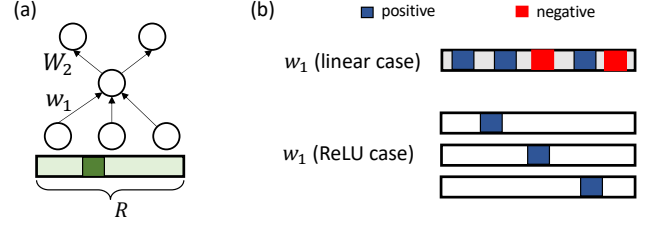


Figure 5. The dynamics can be precisely characterized in one hidden node setting (`ReLU2Layer1Hid`, Sec. 5.2). In linear case, w_1 converges to the maximal eigenvector of X_α ; in ReLU case, w_1 converges to a vector with only one positive entry (Thm. 5).

5.2. Dynamics in One ReLU node

Now we consider the dynamics of one simplest case: a two-layer ReLU network with only 1 hidden node (Fig. 1). In this case, $W_{>1}^\top W_{>1}$ is a scalar and thus $W_2^\top W_2 = \text{tr}(W_2^\top W_2) = 1$. We only need to consider $w_1 \in \mathbb{R}^{n_1}$, which is the only weight vector in the lower layer, under the constraint $\|W_1\|_F = \|w_1\|_2 = 1$ (Eqn. 13). We denote this setting as `ReLU2Layer1Hid`.

The dynamics now becomes very different from linear setting. Under linear network, according to Theorem 3, w_1 converges to the largest eigenvector of $X_\alpha = \mathbb{C}_\alpha[x_1]$. For `ReLU2Layer1Hid`, situation differs drastically:

Theorem 5. *If Assumption 1 holds, then in `ReLU2Layer1Hid`, $w_1 \rightarrow e_m$ for certain m .*

Intuitively, this theorem is achieved by closely tracing the dynamics. When the number of positive entries of w_1 is more than 1, the linear dynamics always hits the boundary of the polytope $w_1 \geq 0$, making one of its entry be zero, and stick to zero due to sticky weight rule. This procedure repeats until there is only one survival positive entry in w_1 .

Overall, this simple case shows a sharp difference between linear case and `ReLU2Layer1Hid`, in which many local optima exist: for any feature m , $w_1 = e_m$ is one local optimal. Which one the training falls into critically affects the properties of per-trained models. For complicated situations like multiple hidden units, getting the exact dynamics becomes hard (if not impossible), and we focus on the energy value \mathcal{E}_α of different θ to determine which one is more likely for the training procedure to converge into.

5.3. Multiple hidden units with non-overlapping receptive fields leads to Feature Compositionality

Now we discuss interaction between different hidden nodes. We consider a non-overlapping 2-layer model in which the receptive field R_k of k -th filter are *disjoint*. Within each R_k , our Assumption 1 applies.

In this case, let $W_1 := \begin{bmatrix} w_{11}^\top & \cdots & 0 \\ 0 & \cdots & w_{1K}^\top \end{bmatrix} \in \mathbb{R}^{K \times Kd}$ be the linear transition matrix from the input to the hidden layer before ReLU activations, where w_{1k} is the k -th filter. We

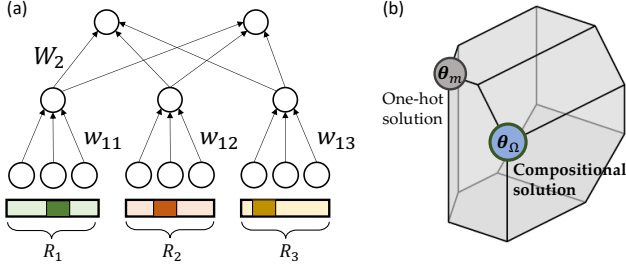


Figure 6. Multiple hidden nodes with non-overlapping receptive fields (ReLU2LayerNoOverlap, Sec. 5.3). In this case, with strong enough data augmentation, solutions/parameters of ReLU2Layer that lead to feature composition are more favorable than those who capture a single dominant feature (Thm. 6).

denote this setting as ReLU2LayerNoOverlap. Such kind of models is used recently in practice, e.g., ViT (Dosovitskiy et al., 2021), MLP-Mixer (Tolstikhin et al., 2021) and SwinTransformer (Liu et al., 2021).

For simplicity of the analysis, we set $\alpha_{ij} = 1/2N(N-1)$ for $i \neq j$ and focus on large batch size (i.e., $N \rightarrow +\infty$). Let $\mathbb{V}[\mathbf{x}]$ be the covariance matrix of the input \mathbf{x} . Note that we have $\sum_{i \neq j} \alpha_{ij} (\mathbf{x}[i] - \mathbf{x}[j])(\mathbf{x}[i] - \mathbf{x}[j])^\top \rightarrow \mathbb{V}[\mathbf{x}]$ and thus:

$$X_\alpha := \mathbb{C}_\alpha[\mathbf{x}] = \mathbb{V}[\mathbf{x}] - D_{\text{aug}}, \quad (14)$$

where the non-negative diagonal matrix D_{aug} represents the effect of data augmentation, due to the augmentation assumption in Assumption 1.

A latent model for feature co-occurrence. We assume a binary latent variable y which governs the observed features. Given y , across blocks k and $k' \neq k$, \mathbf{x}_k and $\mathbf{x}_{k'}$ are independent:

$$\mathbb{P}(\mathbf{x}_k, \mathbf{x}_{k'} | y) = \mathbb{P}(\mathbf{x}_k | y) \mathbb{P}(\mathbf{x}_{k'} | y) \quad (15)$$

Intuitively, this models the data distribution that given the latent variable y , we see feature m_1 a lot in receptive field R_1 , and feature m_2 a lot in receptive field R_2 . That is, feature m_1 and m_2 co-occur. Note that for different value of y , the set of co-occurred features can be different.

Then X_α can be computed analytically. Let Δ be the expected feature difference:

$$\Delta := \mathbb{E}[\mathbf{x} | y = 1] - \mathbb{E}[\mathbf{x} | y = 0] \in \mathbb{R}^{Kd} \quad (16)$$

Intuitively, for each feature m , the associated component in feature difference $|\Delta_m|$ tells how distinctive the feature is, across different value of latent variable y . Let $p_c := \mathbb{P}(y = c)$ be the prior probability of latent variable y , and a block-diagonal matrix $D_V := \text{diag}_k(\mathbb{E}_y \mathbb{V}[\mathbf{x}_k | y]) \in \mathbb{R}^{Kd \times Kd}$:

Lemma 4 (Close form of X_α). *With Eqn. 15 and Eqn. 14,*

$$X_\alpha = p_0 p_1 \Delta \Delta^\top + D_V - D_{\text{aug}} \in \mathbb{R}^{Kd \times Kd} \quad (17)$$

Now let's check whether the learning can capture the *co-occurrence* of features from multiple receptive fields R_k . More concretely, consider parameters/solution $\theta \in \Theta$ of the networks, whose W_1 is only nonzero at specific subset of features. We consider two following cases:

- **One-hot solution** θ_m that capture a single feature. That is, only one entry w_{1km} of one filter w_{1k} is nonzero.
- **Compositional solution** θ_Ω that captures multiple features from different receptive fields. That is, we have an active feature set Ω in which the corresponding weight entries are nonzero.

Note that θ_m and θ_Ω are normalized so that $\theta_m, \theta_\Omega \in \Theta$. Please check proof details of Thm. 6 in SM.

In representation learning, we want to learn θ_Ω which *combines* multiple features from different receptive fields (e.g., $m_1 \in R_1$ and $m_2 \in R_2$) to form a high-level concept at the hidden layer, rather than *relying* features as θ_m does.

A natural question arise: in which situation, the contrastive learning procedure will pick the compositional solution θ_Ω ? Consider the following setting: from each receptive field R_k , we pick the *most salient* feature $m_k^* = \arg \max_{m \in R_k} |\Delta_m|$, where Δ_m is Δ 's component at feature m , and consider the collection of most salient features across different receptive fields: $\Omega = [m_1^*, m_2^*, \dots, m_K^*]$. We also denote the *global salient* feature $m^* = \arg \max_m |\Delta_m|$.

We then show that whether the compositional solution θ_Ω are learned (i.e., emergence of feature composition) critically depends on the degree of data augmentation D_{aug} .

Theorem 6 (Augmentation matters). *Augmentation determines whether feature compositionality is favorable:*

- **(Weak augmentation)** *If $D_{\text{aug}} = \text{diag}(D_V)$ and components of $|\Delta|$ are not identical, then $\mathcal{E}_\alpha(\theta_\Omega) < \mathcal{E}_\alpha(\theta_{m^*})$. That is, one-hot solution θ_{m^*} is preferred over compositional solution θ_Ω ;*
- **(Strong augmentation)** *If $D_{\text{aug}} = \text{diag}(D_V) + \text{diag}^2(\Delta) + \eta I$ for any $\eta \geq 0$ and Δ has ≥ 2 non-zero entries, then $\mathcal{E}_\alpha(\theta_\Omega) > \mathcal{E}_\alpha(\theta_m)$ for any single feature m , including m^* . That is, compositional solution θ_Ω is preferred over any one-hot solution θ_m .*

From the theorem, it is clear that if the augmentation is not strong, then it is possible that a one-hot solution θ_m that captures one single salient feature can suppress the feature composition solution θ_Ω we want the model to learn. This is consistent with the observation in (Chen et al., 2021; Tian et al., 2020b) where the amount of augmentation leads to different learned features, and one feature may overwhelm the other. Here we provide a mathematical mechanism to explain this empirical finding and Sec. 6.2 verifies this insight empirically in STL-10.

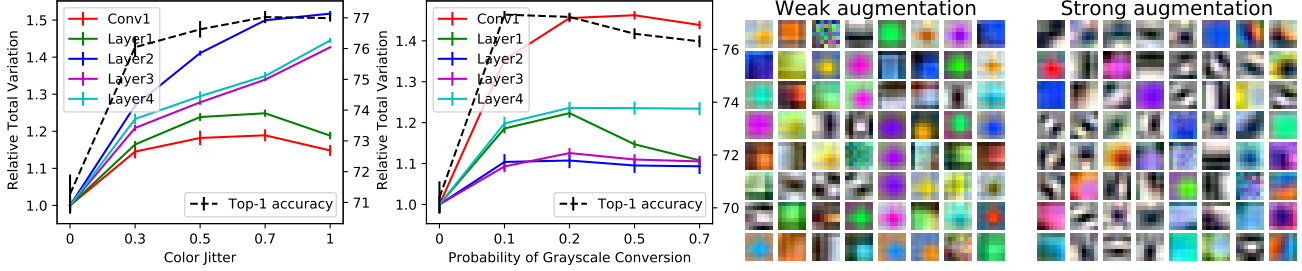


Figure 7. How learned weights changes over different degrees of augmentations. We vary color jitter and probability of image grayscale convention and check the total variation of the learned spatial filters at different ResNet18 layers after training 300 epochs on STL-10. **Left:** With strong augmentation, Top-1 downstream performance (dotted black line) increases, while total variation TV (Eqn. 18) of filters also increases. When Top-1 accuracy plateaus (or drops), TV also plateaus (or drops). Note that for each curve, TV of the first data point is normalized to 1 for easy comparison across layers. **Right:** 7×7 learned convolutional filter at the first layer (before any residual blocks) under weak and strong augmentation. Under weak augmentation, filters tend to detect a specific pixel color, while under strong augmentation, filters become more edge-like, combining nearby image pixels together to construct more complicated visual concepts.

Table 2. Comparison over multiple loss formulations. Top-1 accuracy with linear evaluation protocol. The temperature $\tau = 0.5$. **Bold** is highest performance and **blue** is second highest. Each setting is repeated 5 times with different random seeds.

	100 epochs	300 epochs	500 epochs
<i>CIFAR-10</i>			
\mathcal{L}_{nce}	84.06 \pm 0.30	87.63 \pm 0.13	87.86 \pm 0.12
backprop $\alpha(\theta)$	83.42 \pm 0.25	87.18 \pm 0.19	87.48 \pm 0.21
$\mathcal{P}_g + r_H$	84.27 \pm 0.24	87.75 \pm 0.25	87.92 \pm 0.24
$\mathcal{P}_g + r_\gamma$ ($\gamma = 2$)	83.72 \pm 0.19	87.51 \pm 0.11	87.69 \pm 0.09
$\mathcal{P}_g + r_s$	84.72 \pm 0.10	86.62 \pm 0.17	86.74 \pm 0.15
$\mathcal{P}_g + \text{direct} - \alpha$	85.09 \pm 0.13	88.00 \pm 0.12	88.16 \pm 0.12
<i>STL-10</i>			
\mathcal{L}_{nce}	78.46 \pm 0.24	82.49 \pm 0.26	83.70 \pm 0.12
backprop $\alpha(\theta)$	77.88 \pm 0.17	81.86 \pm 0.30	83.19 \pm 0.16
$\mathcal{P}_g + r_H$	78.53 \pm 0.35	82.62 \pm 0.15	83.74 \pm 0.18
$\mathcal{P}_g + r_\gamma$ ($\gamma = 2$)	78.22 \pm 0.28	82.19 \pm 0.52	83.47 \pm 0.34
$\mathcal{P}_g + r_s$	76.95 \pm 1.06	80.64 \pm 0.77	81.65 \pm 0.59
$\mathcal{P}_g + \text{direct} - \alpha$	79.38 \pm 0.16	82.99 \pm 0.15	84.06 \pm 0.24

6. Experiments

6.1. Comparison of different loss formulations

We evaluate our min-max framework \mathcal{P}_g in CIFAR10 and STL-10 with ResNet18 (He et al., 2016), and compare the downstream performance of multiple losses under our min-max formulation \mathcal{P}_g (Eqn. 28) with regularizers taking the form of $\mathcal{R}(\alpha) = \sum_i \sum_{j \neq i} r(\alpha_{ij})$ with a constraint $\sum_{j \neq i} \alpha_{ij} = 1$. Here r can be different concave functions:

- Entropy regularizer $r_H(\alpha_{ij}) = -2\tau\alpha_{ij} \log \alpha_{ij}$;
- Inverse regularizers $r_\gamma(\alpha_{ij}) = \frac{2\tau}{1-\gamma} \alpha_{ij}^{1-\gamma}$ ($\gamma > 1$).
- Square regularizer $r_s(\alpha_{ij}) = -\frac{\tau}{2} \alpha_{ij}^2$.

Besides, we also compare with the following baselines:

- Original InfoNCE: $\min_{\theta} \mathcal{L}_{nce}(\theta)$;
- backpropagates through $\alpha = \alpha(\theta)$ with respect to θ .
- Directly setting α : $\alpha_{ij} = \frac{\exp(-d_{ij}^p/\tau)}{\sum_{j \neq i} \exp(-d_{ij}^p/\tau)}$ ($p > 1$). Note that $p = 1$ reduces to InfoNCE case (Eqn. 6).

For inverse regularizer r_γ , we pick $\gamma = 2$ and $\tau = 0.5$; for direct-set α , we pick $p = 2$ and $\tau = 0.5$; for square regularizer, we use $\tau = 5$.

The results are shown in Tbl. 2. We can see that (1) back-propagating through $\alpha(\theta)$ is slightly worse, (2) our proposed min-max formulation \mathcal{P}_g works for different regularizers, validating the formulation, (3) using different regularizer leads to comparable or better performance than original InfoNCE \mathcal{L}_{nce} , (4) the pairwise importance α does not even need to come from a minimization process. Instead, we can directly set α based on pairwise distances d_{ij} and d_i .

An interesting pattern is that for strong performance, $\frac{dr}{d\alpha_{ij}}$ should go to $+\infty$ when $\alpha_{ij} \rightarrow 0$. Regularizers that do not satisfy this condition (e.g., squared regularizer r_s) may not work as well. We leave thorough studies as future works.

6.2. Augmentation and structures of learned features

We also empirically verify Theorem 6 in STL-10 dataset, by checking how data augmentation influences the learned features after contrastive learning. We measure the ‘‘structure’’ of filters by computing *total variation* of a spatial filter $w(\xi)$ (ξ is the 2D spatial coordinate):

$$TV(w) := \sum_c \sum_{\xi} \|\nabla w_c(\xi)\|_2 \quad (18)$$

where c is the channel index of the filter. For each convolutional layer, TV is averaged across multiple filters. For ResNet18, we extract the first convolutional layer before any ResNet block (labeled as Conv1 in Fig. 7) and first convolutional layer within each residual block (labeled as LayerX) to compute their TV .

Why total variation? Intuitively, if a filter just focuses on a single feature (e.g., certain color spot), then it tends to be ‘‘blurry’’ in the spatial domain, due to local translational invariance. On the other hand, if a filter captures local

co-occurrence of low-level features, then it must have high-frequency “sharp” component (e.g., an edge detector), while rejecting other competitive co-occurrences. Total variation precisely captures such a trend.

As shown in Fig. 7, with more data augmentation (color jittering and grayscale image conversion), TV at multiple layers increases, suggesting that feature compositionality happens in the trained model, which is consistent with Theorem 6. Furthermore, TV is positively correlated with the downstream performance: with too much data augmentation (e.g., grayscale image conversion rate is too high), downstream performance plateaus (or drops) and TV also plateaus (or drops). Since computing TV on pre-trained weights does not rely on downstream tasks, it can be an (indirect) indicator showing how good the pre-training is.

7. Conclusion and Future Work

We provide a novel game-theoretical perspective of contrastive learning (CL) over loss functions (e.g., InfoNCE) and prove that with deep linear network, the representation learning part is equivalent to Principal Component Analysis (PCA). In addition, we also extend our analysis to representation learning in 2-layer ReLU network, shedding light on the important difference between linear/nonlinear case, and the roles data augmentation plays in the learning process.

Future work. First, the game-theoretical framework turns loss function design into choices of pairwise importance α . This potentially opens a new avenue for loss function design in CL. Second, our analysis on ReLU networks is an important step towards understanding how data augmentation affects learned features. A more general theory with fewer assumptions (e.g., getting rid of Assumption 1) is the next step. Finally, while we have achieved some understanding on representation learning when the pairwise importance α is fixed, in the actual training, α and θ change concurrently. Understanding their interactions is an important next step.

References

- Allen-Zhu, Z., Li, Y., and Liang, Y. Learning and generalization in overparameterized neural networks, going beyond two layers. *arXiv preprint arXiv:1811.04918*, 2018.
- Arora, S., Cohen, N., and Hazan, E. On the optimization of deep networks: Implicit acceleration by overparameterization. In *International Conference on Machine Learning*, pp. 244–253. PMLR, 2018.
- Arora, S., Khandeparkar, H., Khodak, M., Plevrakis, O., and Saunshi, N. A theoretical analysis of contrastive unsupervised representation learning. *arXiv preprint arXiv:1902.09229*, 2019.
- Ba, J. L., Kiros, J. R., and Hinton, G. E. Layer normalization. *arXiv preprint arXiv:1607.06450*, 2016.
- Baldi, P. and Hornik, K. Neural networks and principal component analysis: Learning from examples without local minima. *Neural networks*, 2(1):53–58, 1989.
- Belghazi, M. I., Baratin, A., Rajeshwar, S., Ozair, S., Bengio, Y., Courville, A., and Hjelm, D. Mutual information neural estimation. In *International Conference on Machine Learning*, pp. 531–540. PMLR, 2018.
- Caron, M., Bojanowski, P., Joulin, A., and Douze, M. Deep clustering for unsupervised learning of visual features. In *ECCV*, 2018.
- Caron, M., Misra, I., Mairal, J., Goyal, P., Bojanowski, P., and Joulin, A. Unsupervised learning of visual features by contrasting cluster assignments. In *NeurIPS*, 2020.
- Chen, T., Kornblith, S., Norouzi, M., and Hinton, G. E. A simple framework for contrastive learning of visual representations. 2020.
- Chen, T., Luo, C., and Li, L. Intriguing properties of contrastive losses. In Beygelzimer, A., Dauphin, Y., Liang, P., and Vaughan, J. W. (eds.), *Advances in Neural Information Processing Systems*, 2021. URL <https://openreview.net/forum?id=rYhBGWYm6AU>.
- Chen, X. and He, K. Exploring simple siamese representation learning. In *CVPR*, 2020.
- Coates, A., Ng, A., and Lee, H. An analysis of single-layer networks in unsupervised feature learning. In *International conference on artificial intelligence and statistics*, 2011.
- Coria, J. M., Bredin, H., Ghannay, S., and Rosset, S. A comparison of metric learning loss functions for end-to-end speaker verification. In *International Conference on Statistical Language and Speech Processing*, pp. 137–148. Springer, 2020.
- Dosovitskiy, A., Beyer, L., Kolesnikov, A., Weissenborn, D., Zhai, X., Unterthiner, T., Dehghani, M., Minderer, M., Heigold, G., Gelly, S., et al. An image is worth 16x16 words: Transformers for image recognition at scale. *ICLR*, 2021.
- Du, S., Lee, J., Tian, Y., Singh, A., and Póczos, B. Gradient descent learns one-hidden-layer cnn: Don’t be afraid of spurious local minima. In *International Conference on Machine Learning*, pp. 1339–1348. PMLR, 2018a.
- Du, S. S., Hu, W., and Lee, J. D. Algorithmic regularization in learning deep homogeneous models: Layers are automatically balanced. *arXiv preprint arXiv:1806.00900*, 2018b.

- Fisher, R. A. The use of multiple measurements in taxonomic problems. *Annals of eugenics*, 7(2):179–188, 1936.
- Gemp, I., McWilliams, B., Vernade, C., and Graepel, T. Eigengame: {PCA} as a nash equilibrium. In *International Conference on Learning Representations*, 2021. URL <https://openreview.net/forum?id=NzTU59SYbNq>.
- Grill, J.-B., Strub, F., Altché, F., Tallec, C., Richemond, P. H., Buchatskaya, E., Doersch, C., Pires, B. A., Guo, Z. D., Azar, M. G., et al. Bootstrap your own latent: A new approach to self-supervised learning. *NeurIPS*, 2020.
- Hadsell, R., Chopra, S., and LeCun, Y. Dimensionality reduction by learning an invariant mapping. In *2006 IEEE Computer Society Conference on Computer Vision and Pattern Recognition (CVPR'06)*, volume 2, pp. 1735–1742. IEEE, 2006.
- HaoChen, J. Z., Wei, C., Gaidon, A., and Ma, T. Provable guarantees for self-supervised deep learning with spectral contrastive loss. *NeurIPS*, 2021.
- Hardt, M. and Ma, T. Identity matters in deep learning. *ICLR*, 2017.
- He, K., Zhang, X., Ren, S., and Sun, J. Deep residual learning for image recognition. In *Proceedings of the IEEE conference on computer vision and pattern recognition*, pp. 770–778, 2016.
- He, K., Fan, H., Wu, Y., Xie, S., and Girshick, R. B. Momentum contrast for unsupervised visual representation learning. *2020 IEEE/CVF Conference on Computer Vision and Pattern Recognition (CVPR)*, pp. 9726–9735, 2020.
- Huang, G., Liu, Z., Van Der Maaten, L., and Weinberger, K. Q. Densely connected convolutional networks. In *Proceedings of the IEEE conference on computer vision and pattern recognition*, pp. 4700–4708, 2017.
- Ji, W., Deng, Z., Nakada, R., Zou, J., and Zhang, L. The power of contrast for feature learning: A theoretical analysis. *arXiv preprint arXiv:2110.02473*, 2021.
- Jing, L., Vincent, P., LeCun, Y., and Tian, Y. Understanding dimensional collapse in contrastive self-supervised learning. *ICLR*, 2022.
- Kalantidis, Y., Sariyildiz, M. B., Pion, N., Weinzaepfel, P., and Larlus, D. Hard negative mixing for contrastive learning. *NeurIPS*, 2020.
- Kawaguchi, K. Deep learning without poor local minima. *NeurIPS*, 2016.
- Khosla, P., Teterwak, P., Wang, C., Sarna, A., Tian, Y., Isola, P., Maschinot, A., Liu, C., and Krishnan, D. Supervised contrastive learning. *NeurIPS*, 2020.
- Kokiopoulou, E., Chen, J., and Saad, Y. Trace optimization and eigenproblems in dimension reduction methods. *Numerical Linear Algebra with Applications*, 18(3):565–602, 2011.
- Krizhevsky, A., Hinton, G., et al. Learning multiple layers of features from tiny images. 2009.
- Laurent, T. and Brecht, J. Deep linear networks with arbitrary loss: All local minima are global. In *International conference on machine learning*, pp. 2902–2907. PMLR, 2018.
- Lee, J. D., Lei, Q., Saunshi, N., and Zhuo, J. Predicting what you already know helps: Provable self-supervised learning. *Advances in Neural Information Processing Systems*, 34, 2021.
- Liu, Z., Lin, Y., Cao, Y., Hu, H., Wei, Y., Zhang, Z., Lin, S., and Guo, B. Swin transformer: Hierarchical vision transformer using shifted windows. *ICCV*, 2021.
- Misra, I. and Maaten, L. v. d. Self-supervised learning of pretext-invariant representations. In *CVPR*, 2020.
- Oh Song, H., Xiang, Y., Jegelka, S., and Savarese, S. Deep metric learning via lifted structured feature embedding. In *Proceedings of the IEEE conference on computer vision and pattern recognition*, pp. 4004–4012, 2016.
- Oord, A. v. d., Li, Y., and Vinyals, O. Representation learning with contrastive predictive coding. *arXiv preprint arXiv:1807.03748*, 2018.
- Robinson, J., Chuang, C.-Y., Sra, S., and Jegelka, S. Contrastive learning with hard negative samples. *ICLR*, 2021.
- Safran, I. and Shamir, O. Spurious local minima are common in two-layer relu neural networks. In *International Conference on Machine Learning*, pp. 4433–4441. PMLR, 2018.
- Saxe, A. M., McClelland, J. L., and Ganguli, S. Exact solutions to the nonlinear dynamics of learning in deep linear neural networks. *ICLR*, 2014.
- Schroff, F., Kalenichenko, D., and Philbin, J. Facenet: A unified embedding for face recognition and clustering. In *CVPR*, 2015.
- Sohn, K. Improved deep metric learning with multi-class n-pair loss objective. In *Advances in neural information processing systems*, pp. 1857–1865, 2016.

- Tian, Y. A theoretical framework for deep locally connected relu network. *arXiv preprint arXiv:1809.10829*, 2018.
- Tian, Y. Student specialization in deep relu networks with finite width and input dimension. *ICML*, 2020.
- Tian, Y., Krishnan, D., and Isola, P. Contrastive multiview coding. In *Computer Vision—ECCV 2020: 16th European Conference, Glasgow, UK, August 23–28, 2020, Proceedings, Part XI 16*, pp. 776–794. Springer, 2020a.
- Tian, Y., Sun, C., Poole, B., Krishnan, D., Schmid, C., and Isola, P. What makes for good views for contrastive learning? *NeurIPS*, 2020b.
- Tian, Y., Yu, L., Chen, X., and Ganguli, S. Understanding self-supervised learning with dual deep networks. *arXiv preprint arXiv:2010.00578*, 2020c.
- Tolstikhin, I., Houlsby, N., Kolesnikov, A., Beyer, L., Zhai, X., Unterthiner, T., Yung, J., Keysers, D., Uszkoreit, J., Lucic, M., et al. Mlp-mixer: An all-mlp architecture for vision. *NeurIPS*, 2021.
- Wen, Z. and Li, Y. Toward understanding the feature learning process of self-supervised contrastive learning. *arXiv preprint arXiv:2105.15134*, 2021.
- Wold, S., Esbensen, K., and Geladi, P. Principal component analysis. *Chemometrics and intelligent laboratory systems*, 2(1-3):37–52, 1987.
- Wu, Z., Xiong, Y., Yu, S. X., and Lin, D. Unsupervised feature learning via non-parametric instance discrimination. In *Proceedings of the IEEE conference on computer vision and pattern recognition*, pp. 3733–3742, 2018.
- Xiong, R., Yang, Y., He, D., Zheng, K., Zheng, S., Xing, C., Zhang, H., Lan, Y., Wang, L., and Liu, T. On layer normalization in the transformer architecture. In *International Conference on Machine Learning*, pp. 10524–10533. PMLR, 2020.
- Yeh, C.-H., Hong, C.-Y., Hsu, Y.-C., Liu, T.-L., Chen, Y., and LeCun, Y. Decoupled contrastive learning. *arXiv preprint arXiv:2110.06848*, 2021.
- Zbontar, J., Jing, L., Misra, I., LeCun, Y., and Deny, S. Barlow twins: Self-supervised learning via redundancy reduction. *arXiv preprint arxiv:2103.03230*, 2021.
- Zhou, Y. and Liang, Y. Critical points of linear neural networks: Analytical forms and landscape properties. In *International Conference on Learning Representations*, 2018.

A. Proofs

A.1. Section 3

Theorem 1. For any differential mapping $\mathbf{z} = \mathbf{z}(\mathbf{x}; \boldsymbol{\theta})$, gradient descent of $\mathcal{L}_{\phi, \psi}$ is equivalent to **gradient ascent** of the objective $\mathcal{E}_\alpha(\boldsymbol{\theta}) := \text{tr}(\mathbb{C}_\alpha[\mathbf{z}(\boldsymbol{\theta}), \mathbf{z}(\boldsymbol{\theta})])$:

$$\frac{\partial \mathcal{L}_{\phi, \psi}}{\partial \boldsymbol{\theta}} = -\frac{1}{2} \frac{\partial \mathcal{E}_\alpha}{\partial \boldsymbol{\theta}} \Big|_{\alpha = \alpha(\boldsymbol{\theta})} \quad (19)$$

Here the pairwise importance $\alpha = \alpha(\boldsymbol{\theta}) := \{\alpha_{ij}(\boldsymbol{\theta})\}$ is a function of input batch \mathbf{x} , defined as:

$$\alpha_{ij} := \phi' \left(\sum_{j \neq i} \psi(d_i - d_{ij}) \right) \psi'(d_i - d_{ij}) \geq 0 \quad (20)$$

where $\phi', \psi' \geq 0$ are derivatives of ϕ, ψ . The contrastive covariance $\mathbb{C}_\alpha[\cdot, \cdot]$ is defined as (here $\beta_i := \sum_{j \neq i} \alpha_{ij}$):

$$\begin{aligned} \mathbb{C}_\alpha[\mathbf{a}, \mathbf{b}] &:= \sum_{i \neq j} \alpha_{ij} (\mathbf{a}[i] - \mathbf{a}[j]) (\mathbf{b}[i] - \mathbf{b}[j])^\top \\ &\quad - \sum_{i=1}^N \beta_i (\mathbf{a}[i] - \mathbf{a}[i']) (\mathbf{b}[i] - \mathbf{b}[i'])^\top \end{aligned} \quad (21)$$

Proof. By the definition of gradient descent, we have for any component θ in a high-dimensional vector $\boldsymbol{\theta}$:

$$-\frac{\partial \mathcal{L}}{\partial \theta} = -\sum_{i=1}^N \frac{\partial \mathbf{z}[i]}{\partial \theta} \frac{\partial \mathcal{L}}{\partial \mathbf{z}[i]} + \frac{\partial \mathbf{z}[i']}{\partial \theta} \frac{\partial \mathcal{L}}{\partial \mathbf{z}[i']} \quad (22)$$

Here we use the ‘‘Denominator-layout notation’’ and treat $\frac{\partial \mathcal{L}}{\partial \mathbf{z}[i]}$ as a column vector while $\frac{\partial \mathbf{z}[i]}{\partial \theta}$ as a row vector. Using Lemma 5, we have:

$$-\frac{\partial \mathcal{L}}{\partial \theta} = \mathbb{C}_\alpha \left[\frac{\partial \mathbf{z}}{\partial \theta}, \mathbf{z}^\top \right] \quad (23)$$

On the other hand, treating α as independent variables of $\boldsymbol{\theta}$, we compute (here o_k is the k -th component of \mathbf{z}):

$$\frac{\partial \mathcal{E}_\alpha}{\partial \theta} = \sum_k \mathbb{C}_\alpha \left[\frac{\partial o_k}{\partial \theta}, o_k \right] + \mathbb{C}_\alpha \left[o_k, \frac{\partial o_k}{\partial \theta} \right] \quad (24)$$

For scalar x and y , $\mathbb{C}_\alpha[x, y] = \mathbb{C}_\alpha[y, x]$ and $\sum_k \mathbb{C}_\alpha[a_k, b_k] = \mathbb{C}_\alpha[\mathbf{a}, \mathbf{b}^\top]$ for row vector \mathbf{a} and column vector \mathbf{b} . Therefore,

$$\frac{\partial \mathcal{E}_\alpha}{\partial \theta} = 2\mathbb{C}_\alpha \left[\frac{\partial \mathbf{z}}{\partial \theta}, \mathbf{z}^\top \right] \quad (25)$$

Therefore, we have

$$\frac{\partial \mathcal{E}_\alpha}{\partial \theta} = -2 \frac{\partial \mathcal{L}}{\partial \theta} \quad (26)$$

and the proof is complete. \square

Theorem 2. For InfoNCE loss \mathcal{L}_{nce} with $\epsilon = 0$, the corresponding pairwise importance α (Eqn. 6) is the solution to the minimization problem:

$$\min_{\alpha \geq 0} \mathcal{E}_\alpha(\boldsymbol{\theta}) - \mathcal{R}(\alpha),$$

with the constraint $\sum_{j \neq i} \alpha_{ij} = 1$. Here the regularization $\mathcal{R}(\alpha)$ is the entropy: $\mathcal{R}(\alpha) = \mathcal{R}_H(\alpha) := 2\tau \sum_{i=1}^N H(\alpha_i) = -2\tau \sum_{i=1}^N \sum_{j \neq i} \alpha_{ij} \log \alpha_{ij}$.

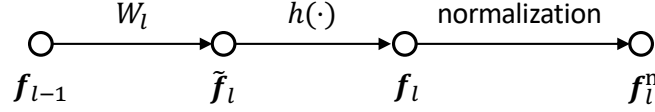


Figure 8. Notations on normalization (Sec. A.2.1).

Proof. We just need to solve the internal minimizer w.r.t. α . Note that each α_i can be optimized independently. Applying Lemma 6 with $c_{ij} = \text{tr}((z[i] - z[j])(z[i] - z[j])^\top) = \|z[i] - z[j]\|_2^2 = 2d_{ij}$, the optimal solution α is:

$$\alpha_{ij} = \frac{\exp(-c_{ij}/2\tau)}{\sum_{j \neq i} \exp(-c_{ij}/2\tau)} = \frac{\exp(-d_{ij}/\tau)}{\sum_{j \neq i} \exp(-d_{ij}/\tau)} \quad (27)$$

which is exactly the coefficients α_{ij} directly computed during minimization of \mathcal{L}_{nce} . \square

Corollary 1. *The minimization of InfoNCE loss \mathcal{L}_{nce} with $\epsilon = 0$ is equivalent to coordinate-wise optimization to the max-min objective $\max_{\theta} \min_{\alpha \geq 0} \mathcal{E}_{\alpha}(\theta) - \mathcal{R}(\alpha)$:*

$$\mathcal{P}_g : \quad \begin{aligned} \alpha_t &= \arg \min_{\alpha \geq 0} \mathcal{E}_{\alpha}(\theta_t) - \mathcal{R}(\alpha) \\ \theta_{t+1} &= \arg \max_{\theta} \mathcal{E}_{\alpha_t}(\theta) \end{aligned} \quad (28)$$

Furthermore, we optimize α analytically (i.e., one step to optimal) while performing one-step gradient ascent for θ .

Proof. The proof naturally follows from the conclusion of Theorem 1 and Theorem 2. \square

A.2. Section 4

Corollary 2 (Representation learning in Deep Linear CL reparameterizes PCA). *When $z = W(\theta)x$ with a constraint $WW^\top = I$, \mathcal{E}_{α} is the objective of Principal Component Analysis (PCA) with reparameterization $W = W(\theta)$:*

$$\max_{\theta} \mathcal{E}_{\alpha}(\theta) = \text{tr}(W(\theta)X_{\alpha}W^\top(\theta)) \quad \text{s.t. } WW^\top = I \quad (29)$$

here $X_{\alpha} := \mathbb{C}_{\alpha}[x]$ is the contrastive covariance of input x .

Proof. Notice that in deep linear setting, $z = W(\theta)x$ where $W(\theta)$ does not depend on specific samples. Therefore, $\mathbb{C}_{\alpha}[z, z] = W(\theta)\mathbb{C}_{\alpha}[x, x]W^\top(\theta) = W(\theta)X_{\alpha}W^\top(\theta)$. \square

Lemma 1. *The training dynamics in DeepLin is:*

$$\dot{W}_l = W_{>l}^\top W_{>l} W_l \mathbb{C}_{\alpha}[f_{l-1}] \quad (30)$$

Proof. We can start from Eqn. 22 directly and takes out $J_{>l}^\top$. This leads to

$$\dot{W}_l = J_{>l}^\top \left(\sum_{i=1}^N \frac{\partial \mathcal{L}}{\partial z[i]} f_{l-1}^\top[i] + \frac{\partial \mathcal{L}}{\partial z[i']} f_{l-1}^\top[i'] \right) = J_{>l}^\top \mathbb{C}_{\alpha}[z, f_{l-1}] \quad (31)$$

Using that $z = J_{\geq l} f_{l-1}$ leads to the conclusion. If the network is linear, then $J_{>l}^\top[i] = J_{>l}^\top$ is a constant. Then we can take the common factor $J_{>l}^\top J_{\geq l}$ out of the summation, yield $\dot{W}_l = J_{>l}^\top J_{\geq l} F_l$. Here $F_l := \mathbb{C}_{\alpha}[f_l]$ is the contrastive covariance at layer l . \square

A.2.1. SECTION 4.2

For this we talk about more general cases where the deep network is nonlinear. Let $h(\cdot)$ be the point-wise activation function and the network architecture looks like the following:

$$z[i] := W_L h(W_{L-1}(h(\dots W_1 \mathbf{x}[i]))) \quad (32)$$

We consider the case where $h(\cdot)$ satisfies the following constraints:

Definition 1 (Reversibility (Tian et al., 2020c) / Homogeneity (Du et al., 2018b)). *The activation function $h(x)$ satisfies $h(x) = h'(x)x$.*

This is satisfied by linear, ReLU, leaky ReLU and many polynomial activations (with an additional constant). With this condition, we have $\mathbf{f}_l[i] = D_l W_l \mathbf{f}_{l-1}[i]$, where $D_l = D_l(\mathbf{x}[i]) := \text{diag}[h'(\mathbf{w}_{lk}^\top \mathbf{f}_{l-1}[i])] \in \mathbb{R}^{n_l \times n_l}$ is a diagonal matrix. For ReLU activation, the diagonal entry of D_l is binary.

Definition 2 (Reversible Layers (Tian et al., 2020c)). *A layer is reversible if there exists $J[i]$ so that $\mathbf{f}_{\text{out}}[i] = J[i]\mathbf{f}_{\text{in}}[i]$ and $\mathbf{g}_{\text{in}}[i] = J^\top[i]\mathbf{g}_{\text{out}}[i]$ for each sample i .*

It is clear that linear layers, ReLU and leaky ReLU are reversible. Lemma 7 tells us that ℓ_2 -normalization and LayerNorm are also reversible.

Lemma 2. *For MLP architecture, if the weight layer W_l is below a ℓ_2 -norm or LayerNorm layer, then $\frac{d}{dt} \|W_l\|_F^2 = 0$.*

Proof. See Lemma 8 that proves more general cases. □

A.2.2. SECTION 4.3

Definition 3 (Aligned-rank-1 solution). *A solution $\theta = \{W_l\}_{l=1}^L$ is called aligned-rank-1, if there exists a set of unit vectors $\{\mathbf{v}_l\}_{l=0}^L$ so that $W_l = \mathbf{v}_l \mathbf{v}_{l-1}^\top$ for $1 \leq l \leq L$.*

Theorem 3 (Representation Learning with DeepLin is PCA). *If $\lambda_{\max}(X_\alpha) > 0$, then for any local maximum $\theta \in \Theta$ of Eqn. 12 whose $W_{>1}^\top W_{>1}$ has distinct maximal eigenvalue:*

- *there exists a set of unit vectors $\{\mathbf{v}_l\}_{l=0}^L$ so that $W_l = \mathbf{v}_l \mathbf{v}_{l-1}^\top$ for $1 \leq l \leq L$, in particular, \mathbf{v}_0 is the unit eigenvector corresponding to $\lambda_{\max}(X_\alpha)$;*
- *θ is global optimal with objective $\mathcal{E}^* = \lambda_{\max}(X_\alpha)$.*

Proof. A necessary condition for θ to be the local maximum is the critical point condition (here λ_{l-1} is some constant):

$$W_{>l}^\top W_{>l} W_l F_{l-1} = \lambda_{l-1} W_l \quad (33)$$

Right multiplying W_l on both sides of the critical point condition for W_l , and taking matrix trace, we have:

$$\mathcal{E}(\theta) = \text{tr}(W_{>l}^\top W_{>l} W_l F_{l-1} W_l^\top) = \text{tr}(\lambda_{l-1} W_l W_l^\top) = \lambda_{l-1} \quad (34)$$

Therefore, all λ_l are the same, denoted as λ , and they are equal to the objective value.

Now let's consider $l = 1$. Then we have:

$$W_{>1}^\top W_{>1} W_1 X = \lambda W_1 \quad (35)$$

Applying $\text{vec}(AXB) = (B^\top \otimes A)\text{vec}(X)$, we have:

$$(X \otimes W_{>1}^\top W_{>1})\text{vec}(W_1) = \lambda \text{vec}(W_1) \quad (36)$$

with the constraint that $\|\text{vec}(W_1)\|_2^2 = \|W_1\|_F^2 = 1$.

We then prove that λ is the largest eigenvalue of $X \otimes W_{>1}^\top W_{>1}$. We prove by contradiction. If not, then $\text{vec}(W_1)$ is not the largest eigenvector, then there is always a direction W_1 can move, while respecting the constraint $\|W_1\|_F = 1$ and keeping W_{-1} fixed, to make $\mathcal{E}(\theta)$ strictly larger. Therefore, for any local maximum θ , λ has to be the largest eigenvalue of $X \otimes W_{>1}^\top W_{>1}$.

Let $\{v_{0m}\}$ be the orthonormal basis of the eigenspace of $\lambda_{\max}(X)$ and \mathbf{u} be the (unique!) unit eigenvector of $W_{>1}^\top W_{>1}$. Then $\text{vec}(W_1) = \sum_m c_m v_{0m} \otimes \mathbf{u}$ where $\sum_m c_m^2 = 1$, or $\text{vec}(W_1) = \mathbf{v}_0 \otimes \mathbf{u}$ where the unit vector $\mathbf{v}_0 := \sum_m c_m v_{0m}$, and $\lambda = \lambda_{\max}(X) \|W_{>1} \mathbf{u}\|_2^2$.

Now we show that $\lambda_{\max}(W_{>1}^\top W_{>1}) = \|W_{>1}\|_2 = 1$. If not, then by Statement 3-4 of Lemma 10, $W_{L:2}$ is not a local maximum and there exists $W'_{L:2}$ in its neighborhood so that (1) $W'_{L:2}$ satisfy the F-norm constraints and (2) $\|W'_{>1}\|_2 > \|W_{>1}\|_2$, or more specifically, $\|W'_{>1} \mathbf{u}\|_2 > \|W_{>1} \mathbf{u}\|_2$. Let $\theta' := \{W'_{L:2}, W_1\}$, we have:

$$\mathcal{J}(\theta') = \text{vec}^\top(W_1)(X \otimes W'_{>1}^\top W_{>1})\text{vec}(W_1) \quad (37)$$

$$= (\mathbf{v}_0^\top \otimes \mathbf{u}^\top)(X \otimes W'_{>1}^\top W_{>1})(\mathbf{v}_0 \otimes \mathbf{u}) \quad (38)$$

$$= \lambda_{\max}(X) \|W'_{>1} \mathbf{u}\|_2^2 \quad (39)$$

$$> \lambda_{\max}(X) \|W_{>1} \mathbf{u}\|_2^2 \quad (40)$$

$$= \lambda = \mathcal{J}(\theta) \quad (41)$$

This means that θ is not a local maximum. Note that θ' is not necessarily a critical point (and Eqn. 33 may not hold for θ'). Therefore, $\lambda_{\max}(W_{>1}^\top W_{>1}) = \|W_{>1}\|_2 = 1$ and thus $\mathcal{E}(\theta) = \lambda = \lambda_{\max}(X)$.

By Statement 1 of Lemma 10, $W_{L:2}$ is aligned-rank-1 and $W_{>1} = \mathbf{v}_L \mathbf{v}_1^\top$ is also a rank-1 matrix. $W_{>1}^\top W_{>1} = \mathbf{v}_1 \mathbf{v}_1^\top$ has a unique maximal eigenvector \mathbf{v}_1 . Therefore $\text{vec}(W_1) = \mathbf{v}_0 \otimes \mathbf{v}_1$, or $W_1 = \mathbf{v}_1 \mathbf{v}_0^\top$. As a result, $\theta := \{W_{L:2}, W_1\}$ is aligned-rank-1.

Finally, since all local maxima have the same objective functions, they are all global maxima. \square

Remarks. Leveraging similar proof techniques, we can also show that with BatchNorm layers, the local maxima are more constrained. From Lemma 11 we know that if each hidden node is covered with BatchNorm, then its fan-in weights are conserved. Therefore, without loss of generality, we could set the per-filter normalization: $\|w_{lk}\|_2 = 1$. In this case we have:

Definition 4 (Aligned-uniform solution). *A solution θ is called aligned-uniform, if it is aligned-rank-1, and $[v_l]_k = \pm 1/\sqrt{n_l}$ for $1 \leq l \leq L-1$. The two end-point unit vectors (\mathbf{v}_0 and \mathbf{v}_L) can still be arbitrary.*

Corollary 3. *If we additionally use per-filter normalization (i.e., $\|w_{lk}\|_2 = 1/\sqrt{n_l}$), then Thm. 3 holds and \mathbf{v}_l is more constrained: $[v_l]_k = \pm 1/\sqrt{n_l}$ for $1 \leq l \leq L-1$.*

Proof. Leveraging Lemma 12 in Theorem 3 yields the conclusion. \square

Remark. We could see that with BatchNorm, the optimization problem is more constrained, and the set of local maxima have less degree of freedom. This makes optimization better behaved.

A.3. Section 5

Lemma 3 (Evaluation of ReLU2Layer). *If Assumption 1 holds, setting $w'_{1k} = \max(w_{1k}, 0)$ won't change the output of ReLU2Layer. Furthermore, if $W_1 \geq 0$, then the formula for linear network $\mathcal{E}_\alpha = \text{tr}(W_2 W_1 X_\alpha W_1^\top W_2^\top)$ still works for ReLU2Layer.*

Proof. For the first part, we just want to prove that if Assumption 1 holds, then a 2-layer ReLU network with weights w_{1k} and W_2 has the same activation as another ReLU network with $w'_{1k} = \max(w_{1k}, 0) \geq 0$ and $W'_2 = W_2$.

We are comparing the two activations:

$$f_{1k} = \max\left(\sum_m w_{1km} x_{km}, 0\right) \quad (42)$$

$$f'_{1k} = \max\left(\sum_m \max(w_{1km}, 0) x_{km}, 0\right) = \sum_m \max(w_{1km}, 0) x_{km} \quad (43)$$

The equality is due to the fact that $x_k \geq 0$ (by nonnegativeness). Now we consider two cases.

Case 1. If all $w_{1k} \geq 0$ then obviously they are identical.

Case 2. If there exists m so that $w_{1km} < 0$. The only situation that the difference could happen is for some specific $x_k[i]$ so that $x_{km}[i] > 0$. By Assumption 1 (one-hotness), for $m' \neq m$, $x_{km'}[i] = 0$ so the gate $d_k[i] = \mathbb{I}(w_{1k}^\top x_k > 0) = 0$. On the other hand, $w_{1k}^\top x_k = 0$ so $d'_k[i] = 0$.

Therefore, in all situations, $f_{1k} = f'_{1k}$.

For the second part, since $W_1 \geq 0$ and all input $x \geq 0$ by non-negativeness, all gates are open and the energy \mathcal{E}_α of `ReLU2Layer` is the same as the linear model. \square

Theorem 4 (Dynamics of `ReLU2Layer`). *If Assumption 1 holds, then the dynamics of `ReLU2Layer` with $w_{1k} \geq 0$ is equivalent to linear dynamics with the **Sticky Weight rule**: any component that reaches 0 stays 0.*

Proof. Let $w_{1k} \geq 0$ be the k -th filter to be considered and $w_{1km} \geq 0$ its m -th component. Consider a linear network with the same weights ($w'_{1k} = w_{1k}$ and $W'_2 = W_2$) with only the ReLU activation removed.

Now we consider the gradient rule of the ReLU network and the corresponding linear network with a sticky weight rule:

$$\dot{w}_{1km} = \sum_i g[i] d_k[i] x_{km}[i] \quad (44)$$

$$\dot{w}'_{1km} = \mathbb{I}(w_{1km} > 0) \sum_i g'[i] x_{km}[i] \quad (45)$$

Thanks to Lemma 13, we know $g[i] = g'[i]$ so we don't need to consider the difference between backpropagated gradient.

In the following, we will show that each summand of the two equations is identical.

Case 1. $x_{km}[i] = 0$. In that case, $g[i] x_{km}[i] = g[i] d_k[i] x_{km}[i] = 0$ regardless of whether the gate $d_k[i]$ is open or closed.

Case 2. $x_{km}[i] > 0$. There are two subcases:

Subcase 1: $d_k[i] = 1$. In this case, the ReLU gating of k -th filter is open, then $g'[i] x_{km}[i] = g[i] x_{km}[i] = g[i] d_k[i] x_{km}[i]$. By Assumption 1 (One-hotness), for other $m' \neq m$, $x_{km'}[i] = 0$, since $d_k[i] = 1$, it must be the case that $w_{1km} > 0$ and thus $\mathbb{I}(w_{1km} > 0) = 1$. So the two summands are identical.

Subcase 2: $d_k[i] = 0$. Then w_{1km} must be 0, otherwise since $x_k \geq 0$ (nonnegativeness), we have $w_{1k}^\top x_k[i] \geq w_{1km} x_{km}[i] > 0$ and the gating of k -th filter must open. Therefore, the two summands are both 0: the ReLU one is because $d_k[i] = 0$ and the linear one is due to $\mathbb{I}(w_{1km} > 0) = 0$. \square

Theorem 5. *If Assumption 1 holds, then in `ReLU2Layer1Hid`, $w_1 \rightarrow e_m$ for certain m .*

Proof. In `ReLU2Layer1Hid`, since there is only one node, we have $X = \mathbb{C}_\alpha[x_1, x_1] = \mathbb{C}_\alpha[x, x]$. By Theorem 4, the dynamics of w_1 is the linear dynamics plus the sticky weight rule, which is:

$$\dot{w}_1 = \text{diag}(w_1 > 0) X w_1 \quad (46)$$

By Lemma 3, the negative parts of w_1 can be removed without changing the result. Let's only consider the nonnegative part of w and remove corresponding rows and columns of X .

Note that the linear dynamics $\dot{w}_1 = X w_1$ will converge to certain maximal eigenvector y (or its scaled version, depending on whether we have norm constraint or not). By Lemma 14, as long as X is not a scalar, y has at least one negative entry. Therefore, by continuity of the trajectory of the linear dynamics, from w_1 to y , the trajectory must cross the boundary of the polytope $w_1 \geq 0$ that require all entries to be nonnegative.

After that, according to the sticky weight rule, in the ReLU dynamics, the corresponding component (say w_{1m}) stays at zero. We can remove the corresponding m -th row and column of X , and the process repeats until X becomes a scalar. Then w_1 converges to that remaining dimension. Since $w_1 \geq 0$, it must be the case that $w_1 \rightarrow e_m$ for some m . \square

Lemma 4 (Close form of X_α). *With Eqn. 15 and Eqn. 14,*

$$X_\alpha = p_0 p_1 \Delta \Delta^\top + D_V - D_{\text{aug}} \in \mathbb{R}^{Kd \times Kd} \quad (47)$$

Proof. Recall that $X_\alpha = \mathbb{V}[\mathbf{x}] - D_{\text{aug}}$. Let $\boldsymbol{\mu}_{kc} := \mathbb{E}[\mathbf{x}_k | y = c]$ and thus $\Delta = [\boldsymbol{\mu}_{k1} - \boldsymbol{\mu}_{k0}] \in \mathbb{R}^{Kd}$. It is easy to see that

$$\mathbb{E}[\mathbf{x}_k] = p_0 \mathbb{E}[\mathbf{x}_k | y = 0] + p_1 \mathbb{E}[\mathbf{x}_k | y = 1] = p_0 \boldsymbol{\mu}_{k0} + p_1 \boldsymbol{\mu}_{k1} \quad (48)$$

Note that for $k \neq k'$ we have $\mathbb{E}[\mathbf{x}_k \mathbf{x}_{k'}^\top | y = c] = \boldsymbol{\mu}_{kc} \boldsymbol{\mu}_{k'c}^\top$ and thus:

$$\text{Cov}(\mathbf{x}_k, \mathbf{x}_{k'}) = \mathbb{E}[\mathbf{x}_k \mathbf{x}_{k'}^\top] - \mathbb{E}[\mathbf{x}_k] \mathbb{E}[\mathbf{x}_{k'}^\top] \quad (49)$$

$$= \sum_{c \in \{0,1\}} p_c \mathbb{E}[\mathbf{x}_k \mathbf{x}_{k'}^\top | y = c] - \left(\sum_{c \in \{0,1\}} p_c \mathbb{E}[\mathbf{x}_k | y = c] \right) \left(\sum_{c \in \{0,1\}} p_c \mathbb{E}[\mathbf{x}_{k'}^\top | y = c] \right) \quad (50)$$

$$= p_0 \boldsymbol{\mu}_{k0} \boldsymbol{\mu}_{k'0}^\top + p_1 \boldsymbol{\mu}_{k1} \boldsymbol{\mu}_{k'1}^\top - (p_0 \boldsymbol{\mu}_{k0} + p_1 \boldsymbol{\mu}_{k1})(p_0 \boldsymbol{\mu}_{k'0} + p_1 \boldsymbol{\mu}_{k'1})^\top \quad (51)$$

$$= p_0 p_1 (\boldsymbol{\mu}_{k0} - \boldsymbol{\mu}_{k1})(\boldsymbol{\mu}_{k'0} - \boldsymbol{\mu}_{k'1})^\top \quad (52)$$

If $k = k'$, then we have

$$\mathbb{E}[\mathbf{x}_k \mathbf{x}_{k'}^\top | y = c] = \mathbb{E}[\mathbf{x}_k \mathbf{x}_k^\top | y = c] = \mathbb{V}[\mathbf{x}_k | y = c] + \boldsymbol{\mu}_{kc} \boldsymbol{\mu}_{kc}^\top \quad (53)$$

Putting them together, we have:

$$\mathbb{V}[\mathbf{x}] = \mathbb{E}[\mathbf{x} \mathbf{x}^\top] - \mathbb{E}[\mathbf{x}] \mathbb{E}[\mathbf{x}^\top] \quad (54)$$

$$= \text{diag}_k(\mathbb{E}_y[\mathbb{V}[\mathbf{x}_k | y]]) + p_0 p_1 \begin{bmatrix} (\boldsymbol{\mu}_{10} - \boldsymbol{\mu}_{11})(\boldsymbol{\mu}_{10} - \boldsymbol{\mu}_{11})^\top & \dots & (\boldsymbol{\mu}_{10} - \boldsymbol{\mu}_{11})(\boldsymbol{\mu}_{K0} - \boldsymbol{\mu}_{K1})^\top \\ \dots & \dots & \dots \\ (\boldsymbol{\mu}_{K0} - \boldsymbol{\mu}_{K1})(\boldsymbol{\mu}_{10} - \boldsymbol{\mu}_{11})^\top & \dots & (\boldsymbol{\mu}_{K0} - \boldsymbol{\mu}_{K1})(\boldsymbol{\mu}_{K0} - \boldsymbol{\mu}_{K1})^\top \end{bmatrix} \quad (55)$$

$$= D_V + p_0 p_1 \Delta \Delta^\top \quad (56)$$

The additional term $\mathbb{V}[\mathbf{x}_k | y = c]$ leads to D_V term on the diagonal. \square

Theorem 6 (Augmentation matters). *Augmentation determines whether feature compositionality is favorable:*

- **(Weak augmentation)** *If $D_{\text{aug}} = \text{diag}(D_V)$ and components of $|\Delta|$ are not identical, then $\mathcal{E}_\alpha(\boldsymbol{\theta}_\Omega) < \mathcal{E}_\alpha(\boldsymbol{\theta}_{m^*})$. That is, one-hot solution $\boldsymbol{\theta}_{m^*}$ is preferred over compositional solution $\boldsymbol{\theta}_\Omega$;*
- **(Strong augmentation)** *If $D_{\text{aug}} = \text{diag}(D_V) + \text{diag}^2(\Delta) + \eta I$ for any $\eta \geq 0$ and Δ has ≥ 2 non-zero entries, then $\mathcal{E}_\alpha(\boldsymbol{\theta}_\Omega) > \mathcal{E}_\alpha(\boldsymbol{\theta}_m)$ for any single feature m , including m^* . That is, compositional solution $\boldsymbol{\theta}_\Omega$ is preferred over any one-hot solution $\boldsymbol{\theta}_m$.*

Proof. We consider solutions where $\text{rank}(W_2) = 1$ (a necessary condition for the solution to be a critical point). In this case, we have $W_2^\top W_2 = \mathbf{s} \mathbf{s}^\top$. When $W_1 \geq 0$ and Assumption 1 holds, the objective function \mathcal{E} for ReLU2Layer is the same as the linear case, and can be written as:

$$\mathcal{E} = \text{tr}(W_2 W_1 X_\alpha W_1^\top W_2^\top) = \mathbf{s}^\top W_1 X_\alpha W_1^\top \mathbf{s} \quad (57)$$

$$= [s_1, \dots, s_K] \begin{bmatrix} \mathbf{w}_{11}^\top & \dots & 0 \\ \dots & \dots & \dots \\ 0 & \dots & \mathbf{w}_{1K}^\top \end{bmatrix} X_\alpha \begin{bmatrix} \mathbf{w}_{11} & \dots & 0 \\ \dots & \dots & \dots \\ 0 & \dots & \mathbf{w}_{1K} \end{bmatrix} \begin{bmatrix} s_1 \\ \dots \\ s_K \end{bmatrix} \quad (58)$$

$$= \begin{bmatrix} s_1 \mathbf{w}_{11} \\ \dots \\ s_K \mathbf{w}_{1K} \end{bmatrix}^\top X_\alpha \begin{bmatrix} s_1 \mathbf{w}_{11} \\ \dots \\ s_K \mathbf{w}_{1K} \end{bmatrix} \quad (59)$$

$$= \sum_{k=1}^K s_k \mathbf{w}_{1k}^\top X_\alpha \mathbf{w}_{1k} s_k \quad (60)$$

Note that the second equality is due to the fact that we are considering ReLU2LayerNoOverlap model.

Now let's construct the compositional solution θ_Ω that corresponds to feature co-occurrence and one-hot solution θ_m :

$$\theta_\Omega : \quad \mathbf{w}_{1k} = \frac{1}{\sqrt{K}} \mathbf{e}_{m_k^*} \geq 0, \quad s_k = \frac{\Delta_{m_k^*}}{\sqrt{\sum_k \Delta_{m_k^*}^2}} \quad (61)$$

$$\theta_m : \quad \mathbf{w}_{1k(m)} = \mathbf{e}_m \geq 0, \quad s_{k(m)} = 1 \quad (62)$$

where $k(m)$ is the receptive field (or hidden-node) index that corresponds to the feature m . It is straightforward to verify that both solutions satisfy the constraint that $\|\mathbf{W}_1\|_F = \|\mathbf{W}_2\|_F = 1$. Therefore, $\theta_\Omega, \theta_m \in \Theta$ (see definition of Θ in Eqn. 13):

Plug in Eqn. 47: $X_\alpha = p_0 p_1 \Delta \Delta^\top + D_V - D_{\text{aug}}$, we consider the following two cases:

Case 1: $D_{\text{aug}} = \text{diag}(D_V)$. In this case, notice that $D_V - D_{\text{aug}}$ has all diagonal zero. So we have:

$$\mathcal{E}(\theta_\Omega) = \frac{p_0 p_1}{K} \left(\sum_k \Delta_{m_k^*} s_k \right)^2 = \frac{p_0 p_1}{K} \sum_{k=1}^K \Delta_{m_k^*}^2 \quad (63)$$

On the other hand, $\mathcal{E}(\theta_{m^*}) = p_0 p_1 \Delta_{m^*}^2$. By definition of m^* (i.e., $|\Delta_{m^*}|$ is the largest) and we know that $\mathcal{E}(\theta_{m^*}) > \mathcal{E}(\theta_\Omega)$.

Case 2: $D_{\text{aug}} = \text{diag}(D_V) + \text{diag}^2(\Delta) + \eta I$ for $\eta \geq 0$. Let $\delta_k := \Delta_{m_k^*}^2 + \eta$. With similar computation, we arrive that

$$\mathcal{E}(\theta_\Omega) = \frac{p_0 p_1}{K} \left(\sum_k \Delta_{m_k^*}^2 - \frac{\sum_k \Delta_{m_k^*}^2 \delta_k}{\sum_k \Delta_{m_k^*}^2} \right) \quad (64)$$

and

$$\mathcal{E}(\theta_m) = p_0 p_1 \left(\Delta_{m_k^*}^2 - \delta_k \right) = -p_0 p_1 \eta \quad (65)$$

Let $a_k := \Delta_{m_k^*}^2 \geq 0$, then $\mathcal{E}(\theta_\Omega)$ can be written as:

$$\mathcal{E}(\theta_\Omega) = \frac{p_0 p_1}{K \sum_k a_k} \left[\left(\sum_k a_k \right)^2 - \sum_k a_k (a_k + \eta) \right] \quad (66)$$

$$= \frac{p_0 p_1}{K \sum_k a_k} \left[\sum_{k \neq k'} a_k a_{k'} - \eta \sum_k a_k \right] \quad (67)$$

$$> -\frac{1}{K} p_0 p_1 \eta \quad (68)$$

$$\geq \mathcal{E}(\theta_m) \quad (69)$$

The first inequality is due to the fact $\{a_k\}$ has ≥ 2 positive entries and $\sum_{k \neq k'} a_k a_{k'} > 0$ is strictly positive. Therefore, $\mathcal{E}(\theta_\Omega) > \mathcal{E}(\theta_m)$, which means that the compositional solution θ_Ω that corresponds to feature co-occurrence has higher energy than the one-hot solution θ_m that only picks certain individual features. \square

Remarks. Note that in the second condition, we actually can prove a stronger case for $D_{\text{aug}} = \text{diag}(D_V) + \text{diag}^2(\Delta) + \text{diag}(\eta)$, where $\eta \in \mathbb{R}^{K^d}$, $\eta \geq 0$ and $\min_{k,m} \eta_{km} > \frac{1}{K} \|\eta\|_\infty$ (i.e., the augmentation is not too imbalanced).

To see this, let $\eta_k := \eta_{m^*(k)} \geq 0$, because

$$\frac{\sum_k a_k \eta_k}{\sum_k a_k} \leq \|\eta\|_\infty \quad (70)$$

Therefore we have:

$$\mathcal{E}(\boldsymbol{\theta}_\Omega) = \frac{p_0 p_1}{K \sum_k a_k} \left[\left(\sum_k a_k \right)^2 - \sum_k a_k (a_k + \eta_k) \right] \quad (71)$$

$$= \frac{p_0 p_1}{K \sum_k a_k} \left[\sum_{k \neq k'} a_k a_{k'} - \sum_k a_k \eta_k \right] \quad (72)$$

$$> -\frac{1}{K} p_0 p_1 \|\boldsymbol{\eta}\|_\infty \quad (73)$$

$$\geq -p_0 p_1 \min_{k,m} \eta_{km} \quad (74)$$

$$\geq \mathcal{E}(\boldsymbol{\theta}_m) \quad (75)$$

B. Other Lemmas

Lemma 5 (Gradient Formula of contrastive Loss (Eqn. 1) (extension of Lemma 2 in (Jing et al., 2022)). *Consider the loss function*

$$\min_{\boldsymbol{\theta}} \mathcal{L}_{\phi, \psi}(\boldsymbol{\theta}) := \sum_{i=1}^N \phi \left(\sum_{j \neq i} \psi(d_i - d_{ij}) \right) \quad (76)$$

Then for any matrix (or vector) variable A , we have:

$$\sum_{i=1}^N \frac{\partial \mathcal{L}_{\phi, \psi}}{\partial \mathbf{z}[i]} A^\top[i] + \frac{\partial \mathcal{L}_{\phi, \psi}}{\partial \mathbf{z}[i']} A^\top[i'] = -\mathbb{C}_\alpha[\mathbf{z}, A] \quad (77)$$

and

$$\sum_{i=1}^N A[i] \frac{\partial \mathcal{L}_{\phi, \psi}}{\partial \mathbf{z}[i]} + A[i'] \frac{\partial \mathcal{L}_{\phi, \psi}}{\partial \mathbf{z}[i']} = -\mathbb{C}_\alpha[A, \mathbf{z}^\top] \quad (78)$$

where $\mathbb{C}_\alpha[\cdot, \cdot]$ is the contrastive covariance defined as:

$$\mathbb{C}_\alpha[\mathbf{x}, \mathbf{y}] := \sum_{i,j=1}^N \alpha_{ij} (\mathbf{x}[i] - \mathbf{x}[j]) (\mathbf{y}[i] - \mathbf{y}[j])^\top - \sum_{i=1}^N \beta_i (\mathbf{x}[i] - \mathbf{x}[i']) (\mathbf{y}[i] - \mathbf{y}[i'])^\top \quad (79)$$

and α is defined as the following:

$$\alpha_{ij} := \phi' \left(\sum_{j \neq i} \psi(d_i - d_{ij}) \right) \psi'(d_i - d_{ij}) \geq 0 \quad (80)$$

where ϕ', ψ' are derivatives of ϕ, ψ .

Proof. Taking derivative of the loss function $\mathcal{L} = \mathcal{L}_{\phi, \psi}$ w.r.t. $\mathbf{z}[i]$ and $\mathbf{z}[i']$, we have:

$$\frac{\partial \mathcal{L}}{\partial \mathbf{z}[i]} = \sum_{j \neq i} \alpha_{ij} (\mathbf{z}[j] - \mathbf{z}[i']) + \sum_{j \neq i} \alpha_{ji} (\mathbf{z}[j] - \mathbf{z}[i]) \quad (81)$$

$$\frac{\partial \mathcal{L}}{\partial \mathbf{z}[i']} = \sum_{j \neq i} \alpha_{ij} (\mathbf{z}[i'] - \mathbf{z}[i]) = \beta_i (\mathbf{z}[i'] - \mathbf{z}[i]) \quad (82)$$

We just need to check the following:

$$\sum_i \left(\sum_{j \neq i} \alpha_{ij} (\mathbf{z}[j] - \mathbf{z}[i']) + \sum_{j \neq i} \alpha_{ji} (\mathbf{z}[j] - \mathbf{z}[i]) \right) A^\top[i] + \sum_i \beta_i (\mathbf{z}[i'] - \mathbf{z}[i]) A^\top[i'] \quad (83)$$

To see this, we only need to check whether the following is true:

$$-\Sigma_0 = \sum_i \left(\sum_{j \neq i} \alpha_{ij} (\mathbf{z}[j] - \mathbf{z}[i']) + \sum_{j \neq i} \alpha_{ji} (\mathbf{z}[j] - \mathbf{z}[i]) \right) A^\top [i] + \sum_i \beta_i (\mathbf{z}[i'] - \mathbf{z}[i]) A^\top [i] \quad (84)$$

which means that

$$-\Sigma_0 = \sum_i \left(\sum_{j \neq i} \alpha_{ij} (\mathbf{z}[j] - \mathbf{z}[i]) + \sum_{j \neq i} \alpha_{ji} (\mathbf{z}[j] - \mathbf{z}[i]) \right) A^\top [i] \quad (85)$$

Since $\alpha_{ii} (\mathbf{z}[i] - \mathbf{z}[i]) = 0$ for arbitrarily defined α_{ii} , j can also take the value of i , this leads to

$$-\Sigma_0 = \sum_{i,j} \alpha_{ij} (\mathbf{z}[j] - \mathbf{z}[i]) A^\top [i] + \sum_{i,j} \alpha_{ji} (\mathbf{z}[j] - \mathbf{z}[i]) A^\top [i] \quad (86)$$

Swapping indices for the second term, we have:

$$-\Sigma_0 = \sum_{i,j} \alpha_{ij} (\mathbf{z}[j] - \mathbf{z}[i]) A^\top [i] + \sum_{i,j} \alpha_{ij} (\mathbf{z}[i] - \mathbf{z}[j]) A^\top [j] \quad (87)$$

$$= \sum_{i,j} \alpha_{ij} (\mathbf{z}[j] - \mathbf{z}[i]) A^\top [i] - \sum_{i,j} \alpha_{ij} (\mathbf{z}[j] - \mathbf{z}[i]) A^\top [j] \quad (88)$$

$$= - \sum_{i,j} \alpha_{ij} (\mathbf{z}[j] - \mathbf{z}[i]) (A^\top [j] - A^\top [i]) \quad (89)$$

and the conclusion follows. \square

Lemma 6. *The following minimization problem:*

$$\min_{p_j} \sum_j c_j p_j - \tau H(p) \quad \text{s.t.} \quad \sum_j p_j = 1 \quad (90)$$

where $H(p) := -\sum_j p_j \log p_j$ is the entropy and $c_j \geq 0$, has close-form solution:

$$p_j = \frac{\exp(-c_j/\tau)}{\sum_{j'} \exp(-c_{j'}/\tau)} \quad (91)$$

Proof. Define the following Lagrangian multiplier:

$$\mathcal{J}(\alpha, \boldsymbol{\theta}) := \sum_j c_j p_j - \tau H(p) + \mu \left(\sum_j p_j - 1 \right) \quad (92)$$

Taking derivative w.r.t p_j and we have:

$$\frac{\partial \mathcal{J}}{\partial p_j} = c_j + \tau (\log p_j + 1) - \mu = 0 \quad (93)$$

which gives the solution

$$p_j = \frac{\exp(-c_j/\tau)}{\sum_{j'} \exp(-c_{j'}/\tau)} \quad (94)$$

\square

Lemma 7. *The normalization function $\mathbf{y} = (\mathbf{x} - \text{mean}(\mathbf{x})) / \|\mathbf{x}\|_2$ has the following forward/backward rule:*

$$\mathbf{y} = J(\mathbf{x})\mathbf{x}, \quad \frac{\partial \mathbf{y}}{\partial \mathbf{x}} = J^\top(\mathbf{x}) \quad (95)$$

where $J(\mathbf{x}) := \frac{1}{\|P_{\mathbf{x}}^\perp\|_2} P_{\mathbf{x},1}^\perp$ is a symmetric matrix. For $\mathbf{y} = \mathbf{x} / \|\mathbf{x}\|_2$, the relationship still holds with $J(\mathbf{x}) = \frac{1}{\|\mathbf{x}\|_2} P_{\mathbf{x}}^\perp$.

Proof. See Theorem 5 in (Tian, 2018). \square

Lemma 8. *Suppose the output of a linear layer (with a weight matrix W_l) connects to a ℓ_2 regularization or LayerNorm through reversible layers, then $\frac{d}{dt}\|W_l\|_F^2 = 0$.*

Proof. From Lemma, for each sample i , we have its gradient before/after the normalization layer (say it is layer m) to be the following:

$$\mathbf{g}_m[i] = J_m^n[i]^\top \mathbf{g}_m^n[i] \quad (96)$$

where $\mathbf{g}_m[i]$ is the gradient after back-propagating through normalization, and $\mathbf{g}_m^n[i]$ is the gradient sending from the top level.

Here $J_m^n[i] = \frac{1}{\|P_{\mathbf{f}_m}^\perp\|_2} P_{\mathbf{f}_m}^\perp$ for LayerNorm and $J_m^n[i] = \frac{1}{\|\mathbf{f}_m[i]\|_2} P_{\mathbf{f}_m}^\perp$ for ℓ_2 normalization. For W_l , its gradient update rule is:

$$\dot{W}_l = \sum_i \tilde{\mathbf{g}}_l[i] \mathbf{f}_{l-1}^\top[i] \quad (97)$$

By reversibility, we know that $\tilde{\mathbf{g}}_l[i] = J_{(\tilde{l}, m)}^\top[i] \mathbf{g}[i]$, where $J_{(\tilde{l}, m)}[i]$ is the Jacobian after the linear layer \tilde{l} till layer m , right before the normalization layer. Therefore, we have:

$$\text{tr}(W_l^\top \dot{W}_l) = \sum_i \text{tr}(W_l^\top J_{(\tilde{l}, m)}^\top[i] J_m^n[i]^\top \mathbf{g}_m^n[i] \mathbf{f}_{l-1}^\top[i]) \quad (98)$$

$$= \sum_i \text{tr}(\mathbf{f}_{l-1}^\top[i] W_l^\top J_{(\tilde{l}, m)}^\top[i] J_m^n[i]^\top \mathbf{g}_m^n[i]) \quad (99)$$

$$= \sum_i \text{tr}(\mathbf{f}_m^\top[i] J_m^n[i]^\top \mathbf{g}_m^n[i]) \quad (100)$$

$$= 0 \quad (101)$$

The last two equality is due to reversibility $\mathbf{f}_m[i] = J_{(\tilde{l}, m)}[i] W_l \mathbf{f}_{l-1}[i]$ and the property of normalization layers: $J_m^n[i] \mathbf{f}_m[i] = 0$, since a vector projected to its own complementary space is always zero $P_{\mathbf{f}_m}^\perp \mathbf{f}_m[i] = 0$.

Then we have

$$\frac{d}{dt}\|W_l\|_F^2 = \frac{d}{dt}\text{tr}(W_l^\top W_l) = \text{tr}(\dot{W}_l^\top W_l) + \text{tr}(W_l^\top \dot{W}_l) = 0 \quad (102)$$

\square

Lemma 9. *For every rank-1 matrix A with $\|A\|_F = 1$, there exists $\|\mathbf{u}\|_2 = \|\mathbf{v}\|_2 = 1$ so that $A = \mathbf{u}\mathbf{v}^\top$.*

Proof. It is clear that there exists \mathbf{u}' and \mathbf{v}' so that $A = \mathbf{u}'\mathbf{v}'^\top$. Since $\|A\|_F = 1$, we have $\text{tr}(AA^\top) = \|\mathbf{u}'\|_2^2 \|\mathbf{v}'\|_2^2 = 1$. Therefore, taking $\mathbf{u} = \mathbf{u}'/\|\mathbf{u}'\|_2$ and $\mathbf{v} = \mathbf{v}'/\|\mathbf{v}'\|_2$, we have $A = \mathbf{u}\mathbf{v}^\top$. \square

Lemma 10. *For the following optimization problem*

$$\max_{\boldsymbol{\theta}} \mathcal{J}(\boldsymbol{\theta}) := \|W_L W_{L-1} \dots W_1\|_2 \quad \text{s.t. } \|W_l\|_F = 1, \quad (103)$$

we have

- (Statement 1) For any solution $\boldsymbol{\theta}$ with $\mathcal{J}(\boldsymbol{\theta}) = 1$, $\boldsymbol{\theta}$ is an aligned rank-1 solution.
- (Statement 2) Any solution $\boldsymbol{\theta}$ with $\mathcal{J}(\boldsymbol{\theta}) = 0$ cannot be a local maximum.
- (Statement 3) Every local maximum is an aligned-rank-1 solution (Def. 3).
- (Statement 4) All local maxima are global with an optimal value of 1.

Proof. Statement 1. Note that we have:

$$\mathcal{J}(\boldsymbol{\theta}) := \|W_L W_{L-1} \dots W_1\|_2 \leq \prod_{l=1}^L \|W_l\|_2 \leq \prod_{l=1}^L \|W_l\|_F = 1 \quad (104)$$

and the equality only holds when all W_l are rank-1. By Lemma 9, for any l , there exists unit vectors $\mathbf{v}'_l, \mathbf{v}_{l-1}$ so that $W_l = \mathbf{v}'_l \mathbf{v}_{l-1}^\top$. To show that they must be aligned (i.e. $\mathbf{v}_l = \pm \mathbf{v}'_l$), we prove by contradiction.

Suppose for some l , $\mathbf{v}'_l \neq \pm \mathbf{v}_l$ and thus $|\mathbf{v}'_l{}^\top \mathbf{v}'_l| < 1$. Then $W_{l+1} W_l = (\mathbf{v}'_{l+1} \mathbf{v}'_l) \mathbf{v}_{l+1} \mathbf{v}_{l-1}^\top$ and $\|W_{l+1} W_l\|_2 \leq \|W_{l+1} W_l\|_F < 1$. Therefore, $\mathcal{J}(\boldsymbol{\theta}) < 1$. Note that for $W_l = \pm \mathbf{v}_l \mathbf{v}_{l-1}^\top$, we can always move around the signs to either \mathbf{v}_0 or \mathbf{v}_L to fit into the definition of aligned-rank-1.

Statement 2. Note that $\mathcal{J}(\boldsymbol{\theta}) = 0$ means that $W_L W_{L-1} \dots W_1 = 0$. Since $\|W_1\|_F = 1$, either $W_{>1} = 0$, or there exists one non-zero row in $W_{>1}$ and a non-zero column in W_1 so that their inner product is 0. For the latter, we can make small change (certain column) of W_1 to W'_1 so that $W_{>1} W'_1 \neq 0$ and thus $\mathcal{J}(\boldsymbol{\theta}') > 0$; for the former, we repeat this until there exists l so that $W_{>l} \neq 0$, then we could slightly change W_l to W'_l so that $W'_{>l-1} = W_{>l} W'_l \neq 0$ and slightly change W_{l-1} to W'_{l-1} so that $W'_{>l-2} \neq 0$, until $W_{>1} W'_1 \neq 0$ and thus $\mathcal{J}(\boldsymbol{\theta}') > 0$. Therefore, $\boldsymbol{\theta}$ cannot be a local maximum.

Statement 3. Suppose $\boldsymbol{\theta}^*$ is a local maximum solution. By Statement 2, $J(\boldsymbol{\theta}^*) > 0$. Since $J(\boldsymbol{\theta}^*)$ is the spectral norm, by its definition, there exists a unit vector \mathbf{u} so that $\|W_L^* W_{L-1}^* \dots W_1^* \mathbf{u}\|_2 = J(\boldsymbol{\theta}^*) > 0$.

Now let $\mathbf{v}'_{L-1} := W_{L-1}^* W_{L-2}^* \dots W_1^* \mathbf{u}$. Note that $\mathbf{v}'_{L-1} \neq 0$ (otherwise $J(\boldsymbol{\theta}^*)$ would be zero). Consider the following optimization subproblem (here we optimize over W_L and treat \mathbf{v}'_{L-1} as a fixed vector).

$$\max_{W_L} \mathcal{J}(W_L; W_{-L}^*) = \|W_L \mathbf{v}'_{L-1}\|_2 \quad \text{s.t. } \|W_L\|_F = 1 \quad (105)$$

By local optimality of $\boldsymbol{\theta}^*$, W_L^* must be the local maximum of Eqn. 105. Note that all critical points of Eqn. 105 must satisfy

$$W_L \mathbf{v}'_{L-1} \mathbf{v}'_{L-1}{}^\top = \lambda W_L \quad (106)$$

for some constant λ . Notice that to satisfy this condition, each row of W_L must be an eigenvector of $\mathbf{v}'_{L-1} \mathbf{v}'_{L-1}{}^\top$. For local maximal solutions, λ is the largest eigenvalue of $\mathbf{v}'_{L-1} \mathbf{v}'_{L-1}{}^\top$, and each row of W_L is the corresponding eigenvector. It is clear that the rank-1 matrix $\mathbf{v}'_{L-1} \mathbf{v}'_{L-1}{}^\top$ has a unique maximum eigenvalue $\|\mathbf{v}'_{L-1}\|_2^2 > 0$ with its corresponding one-dimensional eigenspace span by $\mathbf{v}_{L-1} = \mathbf{v}'_{L-1} / \|\mathbf{v}'_{L-1}\|_2$ (while all other eigenvalues are zeros). Therefore, W_L^* as the local maximum of Eqn. 105, must have:

$$W_L^* = \mathbf{v}_L \mathbf{v}'_{L-1}{}^\top \quad (107)$$

for some $\|\mathbf{v}_L\|_2 = 1$.

Now let $\mathbf{v}'_{L-2} := W_{L-2}^* \dots W_1^* \mathbf{u} \neq 0$. Then $\mathbf{v}'_{L-1} = W_{L-1}^* \mathbf{v}'_{L-2}$. Treating \mathbf{v}'_{L-2} as a fixed vector and varying W_{L-1} and W_L simultaneously, then since $\boldsymbol{\theta}^*$ is a local maximal solution, W_L^* must take the form of Eqn. 110 given any W_{L-1}^* , which means that the objective function now becomes

$$\mathcal{J}(W_{L-1}; W_{-(L-1)}^*) = \|W_L^* \mathbf{v}'_{L-1}\|_2 = \|\mathbf{v}_L \mathbf{v}'_{L-1}{}^\top \mathbf{v}'_{L-1}\|_2 = \|\mathbf{v}'_{L-1}\|_2 = \|W_{L-1} \mathbf{v}'_{L-2}\|_2 \quad (108)$$

and the subproblem becomes:

$$\max_{W_{L-1}} \|W_{L-1} \mathbf{v}'_{L-2}\|_2 \quad \text{s.t. } \|W_{L-1}\|_F = 1 \quad (109)$$

Repeating this process, we know W_{L-1}^* must satisfy:

$$W_{L-1}^* = \mathbf{v}_{L-1} \mathbf{v}'_{L-2}{}^\top \quad (110)$$

for $\mathbf{v}_{L-2} := \mathbf{v}'_{L-2} / \|\mathbf{v}'_{L-2}\|_2$. This procedure can be repeated until W_1 and the prove is complete.

Statement 4. Due to Statement 3, for any local optimal $\boldsymbol{\theta}^*$, we know that $W_L^* W_{L-1}^* \dots W_1^* = \mathbf{v}_L \mathbf{v}_0^\top$, so $\mathcal{J}(\boldsymbol{\theta}^*) = 1$. By the upper bound of the objective (Eqn. 104), we know they are all globally optimal. \square

Lemma 11. $\frac{d}{dt} \|\mathbf{w}_k\|_2^2 = 0$, if node k is under BatchNorm.

Proof. For BN, it is a layer with reversibility on each filter k . We use $\mathbf{f}_k, \mathbf{g}_k \in \mathbb{R}^N$ to represent the activation/gradient at node k in a batch of size N . The forward/backward operation of BN can be written as:

$$\mathbf{f}_k^n = J_k \mathbf{f}_k, \quad \mathbf{g}_k = J_k^\top \mathbf{g}_k^n \quad (111)$$

Here $J_k = J_k^\top = \frac{1}{\|P_1^\perp \mathbf{f}_k\|_2} P_1^\perp \mathbf{f}_{k,1}$ is the Jacobian matrix at each node k .

We check how the weight \mathbf{w}_k changes under BatchNorm. Here we have $\mathbf{f}_k = h(F_{l-1} \mathbf{w}_k)$ where h is a reversible activation and $F_{l-1} \in \mathbb{R}^{N \times n_{l-1}}$ contains all output from the last layer. Then we have:

$$\dot{\mathbf{w}}_k = \sum_i h'_i \mathbf{g}_k[i] \mathbf{f}_{l-1}[i] = F_{l-1}^\top D_k \mathbf{g}_k = F_{l-1}^\top D_k J_k^\top \mathbf{g}_k^n \quad (112)$$

where $D_k := \text{diag}([h'_i]_{i=1}^N) \in \mathbb{R}^{N \times N}$. Due to reversibility, we have $\mathbf{f}_k = h(F_{l-1} \mathbf{w}_k) = D_k F_{l-1} \mathbf{w}_k$. Therefore,

$$\mathbf{w}_k^\top \dot{\mathbf{w}}_k = \mathbf{w}_k^\top F_{l-1}^\top D_k J_k^\top \mathbf{g}_k^n = \mathbf{f}_k^\top J_k^\top \mathbf{g}_k^n = 0 \quad (113)$$

□

Lemma 12 (BatchNorm regularization). *Consider the following optimization problem*

$$\max_{\theta} \mathcal{J}(\theta) := \|W_L W_{L-1} \dots W_1\|_2 \quad \text{s.t.} \quad \|W_L\|_F = 1, \quad \|\mathbf{w}_{lk}\|_2 = 1/\sqrt{n_l} \quad (114)$$

where \mathbf{w}_{lk} are rows of W_l (i.e., weight of the k -th filter at layer l). Then Lemma 10 still holds by replacing aligned-ranked-one with aligned-uniform condition.

Proof. The proof is basically the same. The only difference here is that the sub-problem (Eqn. 109) becomes:

$$\max_{W_l} \|W_l \mathbf{v}'_{l-1}\|_2 \quad \text{s.t.} \quad \|\mathbf{w}_{lk}\|_2 = 1/\sqrt{n_l} \quad (115)$$

for $1 \leq l \leq L-1$. The critical point condition now becomes (here Λ is a diagonal matrix):

$$W_l \mathbf{v}'_{l-1} \mathbf{v}'_{l-1}{}^\top = \Lambda W_l \quad (116)$$

That is, each row of W_l now has a different constant. Since the eigenvalue of $\mathbf{v}'_{l-1} \mathbf{v}'_{l-1}{}^\top$ can only be 0 or 1, and 0 won't work (otherwise the corresponding row of W_l would be a zero vector, violating the row-norm constraint), all diagonal element of λ has to be 1. Therefore, $W_l = \mathbf{v}_l \mathbf{v}_l^\top$. Due to row-normalization, we have $[\mathbf{v}_l]_k = \pm 1/\sqrt{n_l}$ for $1 \leq l \leq L-1$, while \mathbf{v}_L and \mathbf{v}_0 can still take arbitrary unit vector. □

Lemma 13. *If Assumption 1 (Nonnegativeness) holds, then a 2-layer ReLU network with weights $\mathbf{w}_{1k} \geq 0$ and W_2 has the same activations (i.e., $\mathbf{f}_1 = \mathbf{f}'_1$) as its linear network counterpart with the same weights $\mathbf{w}'_{1k} = \mathbf{w}_{1k}$ and $W'_2 = W_2$.*

Proof. Since $W'_2 = W_2$, we only need to prove $\mathbf{f}_1 = \mathbf{f}'_1$. For each filter k , we have its activation $f_{1k} = \max(\sum_m w_{1km} x_{km}, 0)$ and $f'_{1k} = \sum_m w'_{1km} x_{km} = \sum_m w_{1km} x_{km}$. By Assumption 1 (nonnegativeness), all $x_{km} \geq 0$. Since $w_{1km} \geq 0$, $\sum_m w_{1km} x_{km} \geq 0$ and $f_{1k} = f'_{1k}$. □

Lemma 14. *If Assumption 1 holds, $M \geq 2$, \mathbf{x}_1 covers all M modes, and $\alpha_{ij} > 0$, then the maximal eigenvector of X_α always contains at least one negative entry.*

Proof. Let $X_k := C_\alpha[\mathbf{x}_k, \mathbf{x}_k]$. By Lemma 15, all off-diagonal elements of X_k are negative. Then X_k can be written as $X_k = \beta I - X'_k$ for some β where X'_k is a symmetric matrix whose entries are all positive. By Perron–Frobenius theorem, X'_k has a unique maximal eigenvector $\mathbf{u}_k > 0$ (with all positive entries) and its associated positive eigenvalue $\lambda_k > 0$. Therefore, $\mathbf{u}_k > 0$ is also the unique(!) minimal eigenvector of X_k . Since $M \geq 2$, there exists a maximal eigenspace, in which any maximal eigenvector \mathbf{y}_k satisfies $\mathbf{y}_k^\top \mathbf{u}_k = 0$. By Lemma 16, the theorem holds. □

Lemma 15. *If the receptive field R_k satisfies Assumption 1, and the collection of N vectors $\{\mathbf{x}_k[i]\}_{i=1}^N$ contains all M modes, then all off-diagonal elements of $\mathbb{C}_\alpha[\mathbf{x}_k, \mathbf{x}_k]$ are negative.*

Proof. We check every entry of $X_k := \mathbb{C}_\alpha[\mathbf{x}_k, \mathbf{x}_k]$. Note that for off-diagonal element $[X_k]_{ml}$ with $m \neq l$, we have:

$$[X_k]_{ml} = \sum_{ij} \alpha_{ij} (x_{km}[i] - x_{km}[j])(x_{kl}[i] - x_{kl}[j]) - \sum_i \beta_i (x_{km}[i] - x_{km}[i'])(x_{kl}[i] - x_{kl}[i']) \quad (117)$$

Let $A_m := \{i : x_{km}[i] > 0\}$ be the sample set in which the m -th component is strictly positive, and $A_m^c := \{1, 2, \dots, N\} \setminus A_m$ its complement. By Assumption 1 (one-hotness), if $i \in A_m$ then $i \in A_{m'}$ for any $m' \neq m$.

Now we consider several cases for sample i and j :

Case 1, $i, j \in A_m$. Then $i, j \in A_l$ for $l \neq m$. This means that $x_{kl}[i] - x_{kl}[j] = 0$.

Case 2, $i, j \in A_m^c$. Then $x_{km}[i] - x_{km}[j] = 0$.

Case 3, $i \in A_m$ and $j \in A_m^c$. Since $j \in A_m^c$, we have $x_{km}[i] - x_{km}[j] = x_{km}[i] > 0$. On the other hand, since $i \in A_m$, $i \in A_l^c$, we have $x_{kl}[i] - x_{kl}[j] = -x_{kl}[j] \leq 0$. Therefore, $(x_{km}[i] - x_{km}[j])(x_{kl}[i] - x_{kl}[j]) \leq 0$.

Case 4. $i \in A_m^c$ and $j \in A_m$. This is similar to Case 3.

Putting them all together, since $\alpha_{ij} > 0$, we know that

$$\sum_{ij} \alpha_{ij} (x_{km}[i] - x_{km}[j])(x_{kl}[i] - x_{kl}[j]) \leq 0 \quad (118)$$

Furthermore, it is strictly negative since for $i \in A_m$ and $j \in A_l$, we have

$$(x_{km}[i] - x_{km}[j])(x_{kl}[i] - x_{kl}[j]) = -x_{km}[i]x_{kl}[j] < 0 \quad (119)$$

By our assumption that the N vectors $\{\mathbf{x}_k[i]\}_{i=1}^N$ contains all M modes, both A_m and A_l are not empty so this is achievable. For the second summation, by Assumption 1 (Augmentation), either $i, i' \in A_m$ or $i, i' \in A_m^c$, it is always zero for $m \neq l$. \square

Lemma 16. *If $\mathbf{v} > 0$ is an all positive d -dimensional vector, $\mathbf{u}^\top \mathbf{v} = 0$, then*

$$\min_m u_m \leq -\frac{\min_m v_m \|\mathbf{u}\|_\infty}{d - k \|\mathbf{v}\|_\infty} \quad (120)$$

where k is the number of nonnegative entries in \mathbf{u} .

Proof. Let $m_0 := \arg \max_m |u_m|$. If $u_{m_0} = -\|\mathbf{u}\|_\infty = \min_m u_m$ then we have proven the theorem. Otherwise $u_0 := u_{m_0} \geq 0$. u_{m_0} is the largest entry of $\{u_m\}$.

Since $\min_m u_m < 0$, by Rearrangement inequality we have:

$$0 = \mathbf{u}^\top \mathbf{v} = \sum_m u_m v_m \geq \left(\min_m v_m\right) u_0 + (d - k) \left(\max_m v_m\right) \left(\min_m u_m\right) \quad (121)$$

The conclusion follows. \square